Cloning Heterologous Proteins for the *in vitro* Biochemical Characterization of Enzymes Involved in the Synthesis of Cell Wall Polysaccharides

By

ALLISON OBINNA

Thesis
Submitted to Flinders University
for the degree of

Master of Biotechnology
College of Medicine and Public Health
08/07/2024

Principal supervisor: **Dr. Caterina Selva**
Co-supervisor: **Prof. Vincent Bulone**

TABLE OF CONTENTS

ABSTRACT

Both human and plant pathogenic fungi have serious economic, health, and social implications. Rhizopus arrhizus is a filamentous fungus and a common cause of mucormycosis, a severe fungal infection that affects immunocompromised individuals and manifests as fulminant fungal sinusitis, for which there is limited treatment. The cell wall is a vital structural element in fungal organisms, providing both support and protection. It primarily consists of polysaccharides like chitin and glucans that determine fungal integrity and virulence. Our research endeavours to unravel the complexity of the fungal cell wall by shedding light on the functions of cell wall biosynthetic enzymes. These enzymes have diverse biological functions with promising potential as targets for new antifungal strategies.

Specifically, in this project, we aim to clone constructs for the heterologous protein expression and the in vitro biochemical properties of essential cell wall synthetic enzymes, namely GDP-fucose synthase (GFS), fucosyltransferase (FucT), and UDP-N-Acetylglucosamine pyrophosphorylases (UAP1 and UAP2), derived from R. arrhizus, responsible for creating specific polysaccharides that form the fungal cell wall.

Working with clinical R. arrhizus samples from SA Pathology, the genes encoding these enzymes were amplified from cDNA via polymerase chain reaction (PCR). The resulting amplicons were digested with restriction enzymes and ligated into expression vectors. Subsequent transformation of the ligation products into *Escherichia coli* yielded recombinant clones harbouring the genes of interest. UAP1 was successfully cloned, and the recombinant plasmid was sequenced to confirm the integrity of the insert. On the other hand, GFS, FucT, and UAP2 were successfully amplified, digested, ligated, and transformed, but plasmid extraction and sequencing were unsuccessful for these constructs. The inability to sequence these enzymes hinders their further characterization

and limits our understanding of their specific roles in cell wall biosynthesis. Future efforts will focus on optimizing the cloning and expression of these enzymes to enable their biochemical characterization and contribute to a comprehensive understanding of cell wall biosynthesis. Ultimately, we anticipate that these enzymes will catalyse specific reactions crucial for the synthesis of cell wall polysaccharides and represent promising targets for the development of new antifungal strategies.

DECLARATION

I declare that this thesis does not incorporate without acknowledgment any material previously submitted for a degree or diploma in any university, and that the research within will not be submitted for any other future degree or diploma without the permission of Flinders University. I certify that, to the best of my knowledge and belief, it does not contain any previously published or written material by another person, except where appropriately referenced in the text.

Yours sincerely,

Allison P. Obinna

8th July 2024

DEDICATION

This work is dedicated to my family, whose love and support made this achievement possible. To my siblings, for always being there for me. And to my partner, for your unending encouragement and belief in me through this journey. The success of this project wouldn’t be possible without your help.

ACKNOWLEDGEMENTS

I am honestly obliged to a few great people who have been instrumental in my academic life and whose efforts have contributed to making this research see the light of day. First and foremost, I would like to extend very special thanks to my supervisor, Dr. Caterina Selva, whose continuous effort and encouragement were particularly significant in developing my critical thinking ability and perfecting my research abilities. Her complete commitment to my development as a researcher was, and still is, a good example to me. I would also like to express my deep gratitude to my parents, who inculcated into me since very early childhood the value of education in bringing a change in one's life. Through their foresight and sacrifice, they opened my way to avail myself of the opportunities which they themselves had never been given. I do hope I am a disappointment to none of them. I am also grateful to my brother, whose mentorship and support have been a core part of this research work throughout my academic life.

Finally, I recognize that the pursuit of knowledge is never solitary. I have been privileged to learn from the wisdom of many teachers and mentors who have guided me along the way. With humility, I embrace the responsibility to illuminate the path forward for those who will come after me.

LIST OF FIGURES

LIST OF TABLES

Literature Review

Economic, Health, and Social Implications of Fungi

Fungi are eukaryotic organisms closely related to animals. They are also one of the best organic matter decomposers on Earth (Choi et al., 2018). Due to their inability to photosynthesize, fungi obtain nutrients by using enzymatic reactions to break down organic substances. Ecology and the cycle of nutrients therefore largely depend on fungi (Cherney, 2017), as they serve as nature's recycling agents, turning dead organic matter like wood and fallen leaves into essential nutrients (Hoermann et al., 2023).

According to Chen & Chen 2021, we notice that plants grow faster, and it also helps to preserver the ecosystem when that’s an addition of vital nutrients like nitrogen, phosphorus, and carbon to the natural decomposition process. Also, we see that the Fungi has also become more value for industrial and research over the years. For instance, Yeast (Saccharomyces cerevisiae) has been in use for many centuries for the production of foods and drinks, specifically products like beer, bread, and cheese. Furthermore, fungi are as well, active sources of bioactive substances and different enzymes used for many industrial productions like biofuel, pharmaceutical and textile material (Grossart et al., 2019). Because of the presence of certain enzymes, they have been proven useful for research in biotechnology (Adrio & Demain, 2014). Some of these enzymes include lipases from Rhizopus oryzae which is used in the production of detergents and in food processing, amylases from Aspegillus species which is used in starch hydrolysis and also cellulases which is gotten from Trichoderma reesei and is also used for breaking down cellulose (Adrio & Demain, 2014; Grossart et al., 2019). Even with this positive breakthrough of the use of fungi for relevant processes, some fungi can also infect people, plants and animals (Viana, 2021). In agriculture, crop losses brought on by fungus diseases influence world economies and food security, with

an estimated 10–16% of all crop losses worldwide each year attributable to fungus-borne diseases (Fones et al., 2020). An example is wheat rust that can lower wheat yields by up to 70%, and this can directly affect production of food processed with flour like bread and other pastries (Bayer, 2022).

In the health sector, 1.7 billion people globally are afflicted by fungal illnesses, which are a major cause of sickness and death (WHO, 2023). Fungal infections affect both human and animal health, and may vary from minor skin problems like ringworm, which has an impact on the psychological and emotional health of those involved, to serious and sometimes fatal ailments like invasive aspergillosis and candidiasis (CDC, 2023). According to some estimations, invasive aspergillosis has a fatality rate of 30–50% (Brown et al., 2012), which is indicative of the high death rates associated with invasive fungal infections. Fungus infections are on the rise, especially for people with pre-existing health conditions. According to projections, the market for antifungals would expand to a value of $23.9 billion by 2026, which reflects the rising need for treatments (Precedence Research, 2023).

Rhizopus arrhizus

The fugus *Rhizopus arrhizus* which is also known as *R. oryzae* are from the order Mucorales, which is one of the most ancient filamentous terrestrial fungal lineages (Mendoza et al. 2015). They occur naturally in different ecosystems as saprophytic molds, including soil, plant detritus and decomposing organic materials. You can easily find *R. arrhizus* in tropical and subtropical areas because it mostly grows in humid, warm condition (Ribes et al., 2000) and is commonly identified for its importance for both medicinal and industrial use (Kwon-Chung & Sugui, 2013).

This fungi can be used for industrial fermentation, especially when producing certain food items. A good example is the role in the fermented food tempeh, quite popular in Southeastern

Asia. It helps in the breakdown of carbohydrates and proteins during this process, which improves the nutritional content and taste of the product (Hesseltine, 1965). Another important characteristics of this fungus is its ability to produce amylases and lipases, which as very important for food industries and production of biofuels (Pandey et al., 2000). During bioremediation, *R. arrhizus* ca also be used to address environmental pollution, specifically, they are used for remediation of heavy metals from soil and water. Stains from Rhizopus strains can bioaccumulate and detoxify heavy metals, like lead and cadmium, through processes like intracellular complex formation and biosorption (Xu et al., 2019). Another importance of *R. arrhizus* is in the production of fumaric acid, a food acidulant and preservative compound. In some cases, they can be used as a sustainable alternative to petroleum-based diesel, so it is important during the biosynthesis of biodiesel (Kumar et al., 2020). Pectinases, which is one of the enzymes gotten from *R. arrhizus* are important for commercial extraction and clarification of fruit juice and wines (Kashyap et al., 2001).

R. arrhizus is used in medicine to create active metabolites like anticancer and antifungal compounds for drug developments (Fang et al., 2022).

Mucormycosis

Also, *R. arrhizus* can act as opportunistic pathogen to cause mucormycosis, a serious fungal disease commonly referred to as black fungus Mucormycosis is common in certain risk groups (Spellberg et al., 2005). It generally affects people with low immune system, especially those with uncontrolled diabetes, organ transplant recipients, and during treatment of patients who have been diagnosed with neutropenia, with low amount of neutrophils (Ribes et al., 2000; Kauffman, 2015). Skin infections by R. arrhizus, have been reported in natural disasters like tsunamis, cyclones and floods where survivors come in contact with contaminated soil and water (Benedict & Park, 2014). These circumstances are expected to occur more often with increasing extreme weather events due to climate

change. The global incidence of mucormycosis is estimated at over 1 million cases annually (Rauseo et al., 2021), and the Mucorales have been included by the World Health Organization as a ‘high priority’ in the first list of fungal pathogens to guide research, development and public health action (WHO, 2022). Although relatively rare in the general population but has been on the rise, particularly among immunocompromised individuals (Skiada et al., 2020). During the COVID-19 pandemic, there have been reports of an increased incidence of mucormycosis cases, particularly among individuals who were infected with the virus and received treatments such as steroids and immunosuppressive drugs. The compromised immune response associated with severe COVID-19 can make individuals more vulnerable to opportunistic infections like mucormycosis (Singh et al., 2021).

Infection often shows up as fulminant invasive sinusitis, lung infection, or involvement of the skin and soft tissues (Melida et al., 2015). Other symptoms are tissue death, runny nose, one-sided facial pain and swelling, headaches, fevers, and blurred vision in the nose, sinuses, eyes, and brain (Cherney, 2017). Rhinocerebral mucormycosis causes considerable morbidity as a result of the invasion of fungal hyphae into the sinuses, eyes, and brain. For the treatment of this fungal infection, prompt medical intervention is essential, including antifungal medication and surgical debridement (Chakrabarti et al., 2006). However, it is currently hard to treat and manage mucormycosis infections, as they are no clear medical remedy to ensure effective responds to these medical issues (Chakrabarti et al., 2006). Some the reasons why it is very hard to handle includes the ability of the fungal hyphae to rapidly invade the host tissues, also most of the available antifungal drugs prove inefficient in fighting the infection because R. arrhizus can rapidly adapt and evolve drug-resistance (Kwon-Chung & Sugui, 2013). This is some the reason why its mortality rates have a potency of up to 30% to 90%, depending on the site of infection and the patient's overall health (Spellberg et al., 2005).

Cell Wall

The cell wall is present in all fungal species and acts as an external boundary separating the fungal cell from its environment (Free, 2013). It also protects the fungal cell from environmental stressors and host immune responses (Free, 2013). The Fungal cellular walls are vital for the survival and virulence of pathogenic fungi. They are concerned in tactics which includes host tissue invasion and immune evasion and also a possible targets for therapeutic intervention for the reason that disruption of the cellular wall may also cause fungal mobile demise (Latgé, 2007; Munro, 2013).

Here are the main additives of fungal cellular partitions, β-glucans, chitin and glycoproteins. Chitin which is a polymer of N-acetylglucosamine gives the cellular wall its stiffness (Gow et al, 2017). According to Hawks (2017) glycoproteins has a huge role to play in cell signaling and adhesion, while glucans (potentially glucose polymers) help in maintaining the structural strength of the cell wall. Even so, some fungal species may show a different cellular wall architecture. Altered chitin, glucans, and glycoprotein ratios can also vary leading to changes in cell wall structure/function (Gow et al., 2017).

The cell wall of R arrhizus showed some features specific to only this fungus. One different thing with its stratification in the cell walls is that fucans component. Fucans are a group of complex polysaccharides and contain a large number of fucose sugar residues. These novel fucans in R. arrhizus cell walls differentiate them from the rest of FUNGI nature (Deniaud-Bouët et al., 2014). Fucan have yet to be described from R. arrhizus and our preliminary analyses of alkali extracts of both, frozen thawed cell walls and alcohol precipitates of hot water exracts failed to reveal fucans in glucose-containing polymers by 13 C NMR indicating that its composition is specific to this unique Mucorales biology (Deniaud-Bouët et al., 2003). This knowledge further helps to uncover biological aspects of the fungus and maybe even motivates new antifungal targets.

Cell wall synthetic enzymes

Cell wall polysaccharide synthesis is indispensable for cell walls that are necessary for supporting the structural integrity and physiology of cells. During the complex process of cell wall polysaccharide synthesis many enzymes perform the key actions. Monosaccharides, which are the building blocks in general need to be activelyized by converting them to a nucleotide sugar high energy donor. Nucleotide sugars can be metabolized and also build up most of the polysaccharides by glycosyltransferases (Varki et al., 2022). In the current project, we are trying to elucidate the possible role of GDP-fucose synthase and fucosyltransferase in addition to UDP-N-Acetylglucosamine pyrophosphorylase, enzymes responsible for synthesizing necessary polysaccharides of the cell wall during the growth of R. arrhizus. GDP-L-fucose synthase is responsible for the biosynthesis of fucose. As it catalyzes the conversion of GDP-mannose to GDP-fucose, the incorporative building block of fucans and providing the substrate that fucosyltransferases need (Lairson et al., 2008).

Fucosyltransferases (fucTs) are enzymes that transfer fucose residues from GDP-fucose to nucleophilic acceptor molecules such as proteins lipids or glycans (Lairson et al. 2008). UAP1 & UAP2 (UDP-N-acetylglucosamine pyrophosphorylases): these are different important enzyme for the deduction of cadre fence polymountains. These enzymes are responsible for the conversion of UDP-N-acetylglucosamine to UDP-N-acetylglucosamine-1-phosphate an important precursor molecule in chitin biosynthesis--the major structural polysaccharide of fungal cell walls (Vollmer et al. 2006). We hope that the precise role and mechanisms of action of UAP2 remain clearly defined throughout the work and here we focused on the production of these genes from R. arrhizus. To increase the accuracy of

further studies, we need to clone these genes. When this genes are expressed and transformed, it makes it easier to perform a range of other experiment that would help to further explain their individual roles in cell wall polysaccharide synthesis.

RESEARCH GAP

The increases high mortality rate and limited options of treatment are some of the reasons why it's important to research on mucormycosis is very important is because of its growing cases, high mortality rates, and limited treatment options. The need to better understand *R. arrhizus* to identify suitable targets for the development of effective antifungal strategies specific to the Mucorales is obvious and aligns our research with global health priorities. Targeting enzymes involved in cell wall formation and integrity presents a promising approach to affect fungal growth and holds potential for improving the management of mucormycosis and benefiting both patient outcome and healthcare systems. By starting with the cloning and characterization of these genes, we lay the groundwork for comprehensive studies that will ultimately enhance understanding of the biosynthesis of fungal cell wall polysaccharides. This knowledge can contribute to the development of new strategies for targeting fungal pathogens.

HYPOTHESIS

In this project, it is hypothesized that characterizing the cell wall synthetic enzymes GDP-fucose synthase (GFS), fucosyltransferase (FucT), and UDP-N-Acetylglucosamine pyrophosphorylases (UAP1 and UAP2) from *R. arrhizus* will provide crucial information as potential targets for new antifungal strategies.

OBJECTIVE

The overarching objective of this project is to validate the specific roles and mechanisms of GFS, FucT, and UAP1 & UAP2 in cell wall biosynthesis. To do this, our current focus is on cloning these genes from *R. arrhizus*.

AIMS

1. Amplify GFS, FucT, UAP1 and UAP2 from *R. arrhizus* cDNA.
2. Clone genes into expression vector for heterologous protein expression.
3. Validate constructs generated.

MATERIALS & METHODS

In this study, we cloned the plasmids for heterologous expression purification and *in vitro* biochemical characterization of enzymes involved in the synthesis of fungal cell wall polysaccharides, with a specific focus on GDP-fucose synthase (GFS), UDP-N-Acetylglucosamine pyrophosphorylase (UAP1 and UAP2), and fucosyltransferase (FucT). The comprehensive experimental design encompassed multiple steps, including amplification, gel electrophoresis, restriction enzyme digestion, ligation, transformation in bacterial competent cells, plasmid extraction, plasmid verification, and glycerol stocks for long-term storage.

Rhizopus arrhizus cultures

The *Rhizopus arrhizus* strain used in this study was kindly provided by Dr. Sarah Kidd from SA Pathology. It was isolated from necrotized subcutaneous tissue of a patient, highlighting its clinical relevance and ability to cause invasive mucormycosis infections in humans. We are grateful to Dr. Kidd for sharing this clinically important strain, which enabled us to investigate the virulence factors and pathogenesis mechanisms employed by this opportunistic fungal pathogen.

Media preparation – LB, LBA

To prepare LB media, I first decided on the total volume I wanted to make. For this research I decided to make 300 mL. I ensured the volume was no more than 75% of the container volume to allow for mixing and headspace. I measured out 200 mL of Milli-Q water in a beaker. I then calculated and weighed out the appropriate amount of LB broth powder (Sigma-Aldrich) based on the desired final volume (25g/L). I added the powders to the beaker of water and dissolved them completely using a magnetic stir bar and stir plate. Once fully dissolved, I

poured the solution into a graduated cylinder and brought it up to the final volume of 300 mL with additional Milli-Q water. I then transferred the LB media into an appropriately sized bottle for autoclaving at 121°C for 35 minutes.

For LBA, I followed the same steps as for LB media until the final volume was reached. Before pouring the LB into the storage bottle, I calculated and directly added the required amount of agar into the bottle. I swirled the bottle to mix in the agar thoroughly. This prevented any agar clumping before autoclaving. The LBA was then autoclaved using the same conditions as stated above.

Amplification – cloning, colony PCR

Polymerase Chain Reaction (PCR) using Q5 DNA polymerase (New England Biolabs) was performed to amplify the target genes GDP-fucose synthase (GFS), UDP-N-Acetylglucosamine pyrophosphorylase (UAP1 and UAP2), and fucosyltransferase (FucT). The 25 µL PCR master mix consisted of 5 µL 5X Q5 reaction buffer, 0.5 µL 10 mM dNTPs, 1.25 µL 10 µM forward primer, 1.25 µL 10 µM reverse primer, 10 ng fungal cDNA as template, 0.25 µL Q5 DNA polymerase, and 13.75 µL nuclease-free water. The thermocycling conditions were initial denaturation at 98°C for 30 seconds, followed by 30 cycles of denaturation at 98°C for 10 seconds, annealing at 50-65°C for 20 seconds, and extension at 72°C for 30 seconds/kb, with a final extension at 72°C for 2 minutes.

Primers used for amplification are listed in **Table 1**.

The PCR products were analyzed by agarose gel electrophoresis using a 1% agarose gel in 1x TAE buffer. 5 µL of PCR product mixed with 1 µL 6X gel loading dye was loaded into each well alongside 5ul of a 1 Kb Plus DNA ladder (New England BioLabs). The gel was run at 100V for 30 minutes and visualized under UV light. The concentration of the PCR products was quantified using a Nanodrop spectrophotometer (Thermo Fisher Scientific)

by measuring the absorbance at 260 nm. 1 µL of each PCR product was loaded onto the Nanodrop pedestal, and the nucleic acid concentration was calculated based on the absorbance using the instrument's software.

To confirm plasmid presence, colony PCR was performed on transformed Escherichia coli colonies. A sterile pipette tip was used to pick a single bacterial colony and transfer a small amount of cells into a PCR tube containing the PCR master mix described above, but using plasmid-specific primers instead of the gene-specific primers. The thermocycling conditions were the same as for the original PCR reactions. The colony PCR products were analyzed by agarose gel electrophoresis as described previously.

Gel Purification

To purify DNA fragments from PCR and enzymatic reactions, I used the New England BioLabs. Inc. NucleoSpin Gel and PCR Clean-up kit following the manufacturer's protocol.

For small sample volumes under 30 µL I added Milli-Q water to a final volume of 100 µL. I then added 2 volumes of Buffer NTI to 1 volume of PCR reaction (e.g. 100 µL PCR sample + 200 µL Buffer NTI) to adjust binding conditions. This allowed removal of small fragments like primer dimers. Next, the sample was loaded to a binding column and the DNA was bound to the silica membrane in the column. The silica membrane was washed twice with 700 µL of Buffer NT3. Residual wash buffer was removed by centrifugation for 1 minute at 11,000 x g. The column was placed into a clean 1.5 mL microcentrifuge tube and the DNA was eluted by adding 50 µL of Buffer NE, incubating at room temperature for 1 minute, then centrifuging for 1 minute at 11,000 x g. The purified DNA was now ready for downstream applications.

Digestion – cloning, plasmid check

For cloning experiments and verifying plasmid constructs, I performed enzymatic digestion of DNA. For cloning, I used restriction enzymes to linearize the plasmid and generate compatible ends for ligation in the insert DNA.

For cloning, I digested approximately 1 µg of the DNA. The reactions also included, 2 µL of each restriction enzyme BamHI & NotI, and the 2 µL of reaction buffer recommended by the enzyme supplier and 2 µL of MQ water. The total volume was adjusted to 20 µL with nuclease-free water. The digestion reactions were incubated at 37°C for 1 hour.

The digested DNA was analyzed by agarose gel electrophoresis. Successful restriction digestion was verified by visualizing the linearized plasmid backbone and insert DNA fragments at the expected sizes. The digested DNA was then purified and concentrated using a PCR cleanup kit as mentioned above prior to ligation reactions.

To verify plasmid constructs, diagnostic restriction digests were performed on miniprep DNA using enzymes flanking the insert or multiple sites within the vector. The fragments were separated on gel electrophoresis and compared to the expected banding patterns to confirm successful cloning.

Ligation

The vector and insert fragments obtained through restriction enzyme digestion and gel purification underwent ligation reaction with BamHI & NotI from New England BioLabs.Inc to catalyse the formation of phosphodiester bonds between the 5' phosphate and 3' hydroxyl ends of the vector and insert DNA fragments. A 1:3 molar ratio of vector to insert DNA was used as calculated by NEBioCalculator (https://nebiocalculator.neb.com/#!/ligation). Specifically, I used 60 pmol of insert DNA and 20 pmol of vector DNA. The ligation reaction also contained 1X T4 DNA ligase buffer and T4 DNA ligase in a final volume of 20 µL. After adding the T4 DNA ligase last, I gently mixed the reaction by pipetting up and down and briefly centrifuged. For cohesive end ligation, I incubated the reaction overnight at 16°C. Following incubation, the T4 DNA ligase was heat inactivated at 65°C for 10 minutes then chilled on ice. 1-5 µL of the ligation reaction were used for transformation into 50 µL of DH5-alpha Escherichia coli competent cells for propagation of the ligated plasmids.

Transformation

To introduce the ligated plasmid DNA into DH5- alpha E. coli, I followed a heat shock transformation protocol. First, I thawed the competent cells on ice. For each transformation, I aliquoted 25 µL of cells to a chilled microcentrifuge tube. I then added 5 µL of ligation reaction to the competent cells and gently mixed by flicking the tube. The tubes were incubated on ice for 30 minutes. After chilling, I performed the heat shock by placing the tubes in a 42°C water bath for exactly 30 seconds. The tubes were then immediately returned to ice for 2 minutes. Next, 250 µL of LB medium was added to each tube. The tubes were shaken horizontally at 225 rpm for 60 minutes at 37°C to allow recovery and expression of the antibiotic resistance gene. Finally, 50 µL, 100 µL, and 125 µL of each transformation reaction were spread onto separate selective LB agar plates containing 100 µg/mL ampicillin. The plates were incubated overnight at 37°C.

The following day, I screened for transformants by checking for colony growth on the selective plates. Individual colonies were picked for colony PCR to confirm the presence of the plasmid with the insert. Colonies containing the desired clone were used to inoculate LB cultures for plasmid extraction.

Plasmid Extraction (Miniprep)

Inside a biosafety cabinet, I first labeled 50mL culture tubes. I then aliquoted 12 mL of LBA medium into each tube. Since the plasmids contained an ampicillin resistance gene, I added ampicillin to a final concentration of 100 µg/mL in each tube to select for plasmid-containing cells. Next, I used a sterile inoculation loop to pick a single transformed colony from my transformation plate and transferred it to the LB tube. I dispersed the cells into the medium by gently swirling. The inoculated tubes were incubated overnight at 37°C with shaking at 225 rpm to allow the cells to propagate. This achieved exponential growth phase for maximum plasmid yield. After the overnight culture, the tubes were removed from the incubator. If the LB broth appeared turbid due to bacterial cell growth, the cultures were then ready for plasmid extraction to isolate the amplified plasmids.

To isolate plasmid DNA from my transformed E. coli cultures, I used the Monarch Plasmid Miniprep kit from New England BioLabs.inc following manufacturer's instructions. I began by pelleting the cells by centrifuging 1-5 mL of saturated LB culture at 11,000 x g for 30 seconds. I completely resuspended the cell pellets in 250 µL Buffer A1 by vortexing. For cell lysis, I added 250 µL Buffer A2 and gently mixed by inverting 6-8 times. After incubating the tubes at room temperature until the lysates cleared, I added 300 µL Buffer A3 and inverted until the samples were completely colorless. This indicated full neutralization had occurred. I clarified the lysates by centrifuging at 11,000 x g for 1 minute. I loaded up to 700 µL of the supernatants onto NucleoSpin columns and centrifuged for 1 minute to bind the plasmid DNA. Any remaining lysate was also loaded

and centrifuged. To wash away contaminants, I first added 600 µL ethanol-supplemented Buffer A4 and centrifuged the columns and performed an additional wash with Buffer AW. The columns were centrifuged dry before proceeding to elution. To elute my plasmid DNA, I added 50 µL Buffer AE to the columns and let sit for 1 minute at room temperature. After centrifuging for 1 minute, I obtained purified plasmid ready for downstream applications.

Sanger sequencing

Sanger sequencing played a lead role in confirming the validity of the cloned DNA fragments, with a specific focus on validating gene and plasmid sequences. The sequencing reaction setup was prepared comprising 1 µl of primer to initiate the sequencing reaction, 10-30 ng of DNA template, and water up to a final volume of in 12 µl. Samples were then sent to the Australian Genome Research Facility (AGRF) for Sanger sequencing by capillary electrophoresis.

Glycerol stocks

To ensure the long-term preservation of the successful clones, glycerol stocks were prepared for storage at -80°C. From the overnight culture used for plasmid extraction, 800 µL of the bacterial culture was mixed with 200 µL of sterile 80% glycerol in a cryovial. The glycerol stock mixture was gently inverted several times to ensure homogeneity and then immediately frozen at -80°C.

RESULTS

Preparation of pYES2/CT vector

The pYES2/CT vector (**Figure 1**) was chosen for this experiment because it is a versatile expression vector for the production of recombinant proteins in the yeast *Saccharomyces cerevisiae*. This vector contains several key components that facilitate protein expression and purification:

1) Galactose-inducible GAL1 promoter which allows tight regulation of the cloned gene expression by induction with galactose.
2) C-terminal tags encoding the peptides like V5 epitope and 6xHis which enable detection and purification of the expressed protein.
3) URA3 marker which provides auxotrophic selection for transformants in uracil-deficient media.
4) Ampicillin resistance gene to allow selection of the plasmid in *Escherichia coli* during cloning steps.
5) pUC origin which permits high-copy replication in *E. coli*.

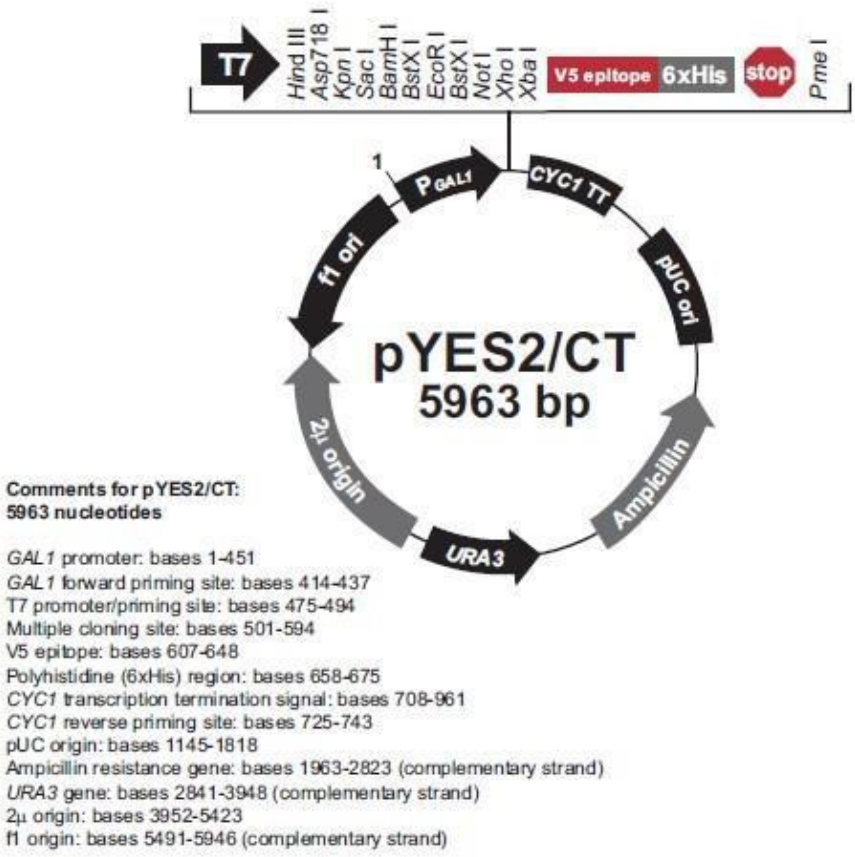

Figure 1. pYES2/CT vector map. Figure 1 shows a map of the pYES2/CT vector showing key features such as the GAL1 promoter, C-terminal tags (V5 epitope and 6xHis), URA3 marker, ampicillin resistance gene, and pUC origin.

Based on **Figure 2** showing the multiple cloning site (MCS) of the pYES2/CT vector, the restriction enzymes BamH I and Not I will be used for cloning. These enzymes create compatible sticky ends that can be ligated to the insert DNA fragment containing the gene of interest.

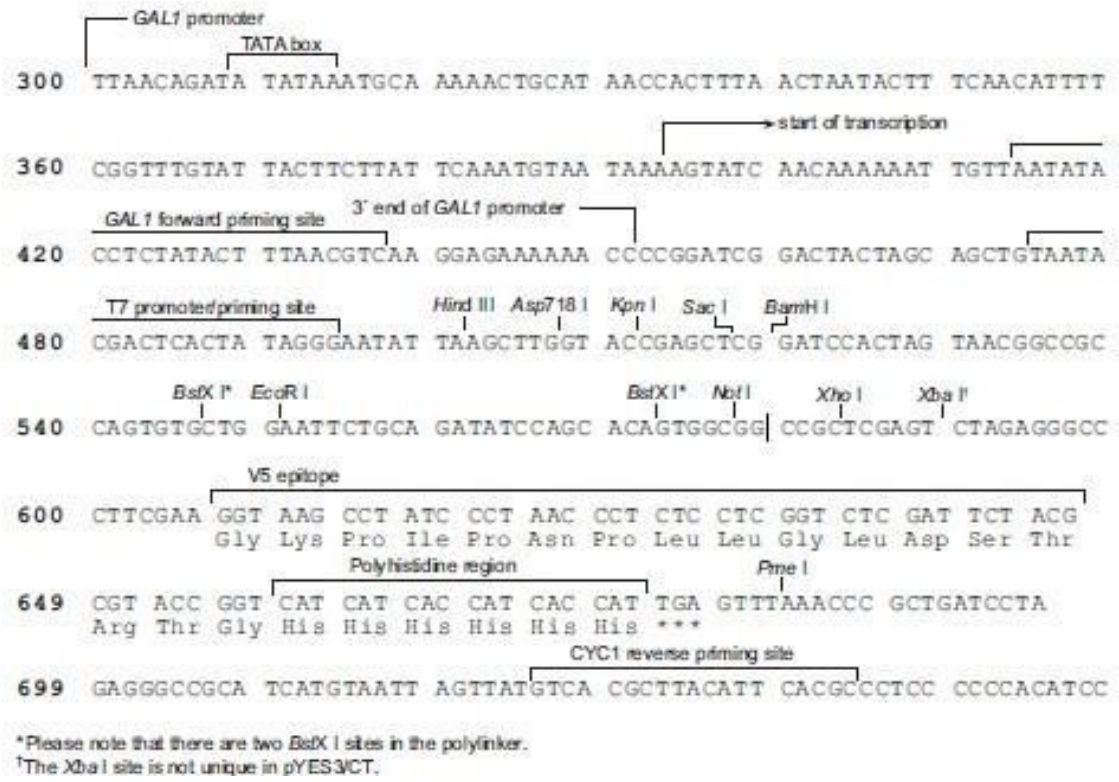

*Please note that there are two *BstX* I sites in the polylinker.
†The *Xba* I site is not unique in pYES3/CT.

Figure 2. pYES2/CT multiple cloning site. Figure 2 shows Multiple cloning site (MCS) of the pYES2/CT vector. The restriction enzymes BamHI and NotI are shown, which were used for cloning the insert DNA fragment.

The pYES2/CT vector was linearized with the restriction enzymes BamHI and NotI to create compatible sticky ends for ligation with the insert DNA fragment. As shown in Figure 3, the gel image of the digested pYES2/CT vector reveals a single band corresponding to the linearized plasmid backbone of the expected size (approximately 5.9 kb).

This implies that there's a successful double digestion with BamHI and NotI as preparation of the vector for ligation with the insert DNA. However, the linearized vector went through purification with the use of commercial purification kit after digestion to remove buffer components, enzymes, and unwanted DNA fragments. Then we had to qualify the purified vector with a spectrophotometer to get its concentration, while using a precise amount was

used in subsequent ligation reactions. We found the purified vector to be 45 ng/µL, which is required for ligation with the insert DNA fragment.

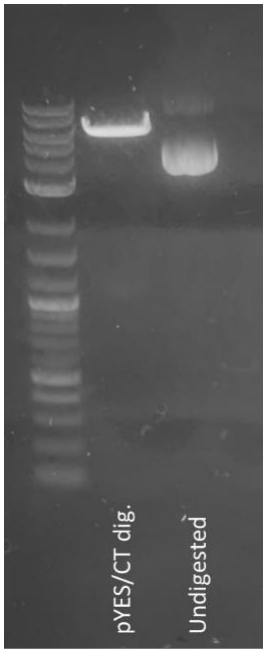

Figure 3. pYES2/CT vector digestion of Gel image. Figure 3 shows Agarose gel electrophoresis image showing the pYES2/CT vector linearized with BamHI and NotI. A single band corresponding to the linearized plasmid backbone (~5.9 kb) confirms successful digestion.

Cloning of GDP-Fucose synthase (GFS)

GDP-fucose synthase was chosen for our studies because it is an enzyme involved in the biosynthesis of GDP-fucose, a precursor for the formation of fucans, fucose-containing polysaccharides in fungal cell walls. It catalyzes the reaction of converting GDP-mannose to GDP-fucose through a two-step process (**Figure 4**): GDP-4-dehydro-6-deoxy-D-mannose + NADPH + H^+ ⇌ GDP-L-fucose + $NADP^+$

Figure removed due to copyright restriction.

Figure 4. Reaction catalyzed by GFS from https://www.uniprot.org/uniprot/Q13630.

Figure 4 shows diagram of the reaction catalyzed by GDP-Fucose synthase (GFS), converting GDP-mannose to GDP-fucose.

To clone GFS, the entire coding sequence was amplified from the cDNA of *R. arrhizus* using primers RO-193 and RO-194. As shown in **Table 1**, the primers contain BamHI and NotI restriction sites for subsequent cloning into the PYES2/CT vector. From the cDNA amplification, a band of 982 bp was expected. This was confirmed by gel electrophoresis (**Figure 5**).

Table 1. List of primers used for amplification of all genes.

Gene	FW	REV	Amplicon
GFS	RO_193 CATGGATCCTATGTCAGTTATTCTTGTCACTGG	RO_194 TTGCGGCCGCGATTTACGACAGTTGTCATAGTTTTC	963 bp
FucT	RO_199 CATGGATCCTATGGACGTCGTCAATCG	RO_200 TTGCGGCCGCGAAACATAGACATGTTCCTGTTTA	918 bp
UAP1	RO_195 CATGGATCCTATGACTGTCTCCTCACTTCTTCC	RO_196 TTGCGGCCGCGAATGAGCAAAACGAATCAAGTCTTCC	1503 bp
UAP2	RO_197 CATGGATCCTATGACCGTTTCTTCACTTCTG	RO_198 TTGCGGCCGCGAATGAGCAAAACGAATTAAATCTTC	1509 bp

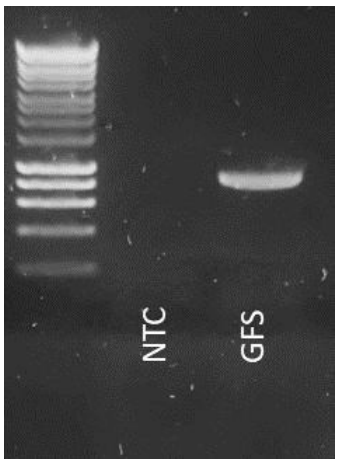

Figure 5. Gel image for PCR of GFS gene. Figure 5 shows agarose gel electrophoresis image showing the PCR amplification of the GFS gene. A single band of 982 bp confirms successful amplification.

Subsequent to amplification, the GFS gene was purified from gel and quantified by Nanodrop, obtaining a concentration of 45 ng/μL. The purified GFS gene was subjected to Sanger sequencing at the Australian Genome Research Facility (AGRF) to confirm the sequence (**Figure 6**).

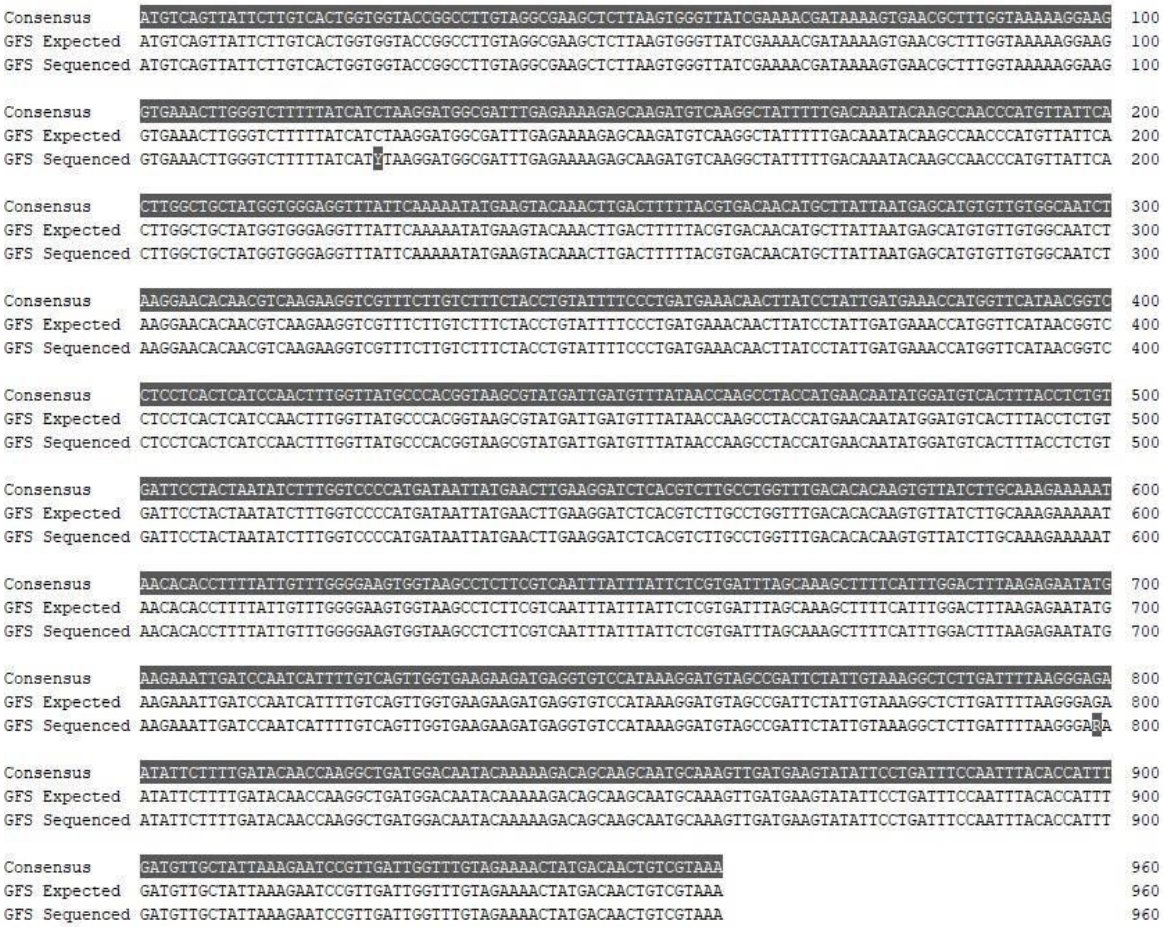

Figure 6. Alignment of GFS sequence. Figure 6 shows alignment of the GFS sequence obtained from Sanger sequencing, showing the amplified gene and the detected SNPs compared to the reference genome.

The sequencing revealed that the correct gene had been amplified, and it contained 2 single nucleotide polymorphisms (SNPs) compared to the reference genome.

1 µg of material was used for restriction digestion with restriction enzymes BamH I and Not I to generate overhangs compatible with the expression vector pYES2/CT. The digested GFS gene fragment was purified, and quantified. Approximately 60 pmol of purified GFS gene were ligated with 20 pmol of linearized vector backbone. The ligation mixture containing the recombinant GFS vector, named pYES2/CT-GFS was transformed into DH5-Alpha cells chemically competent *E.coli* cells. The transformation process introduced the recombinant DNA into the host cells, enabling them to propagate and express the desired GFS gene. Following overnight growth at 37°C on selective media containing ampicillin at 100 µg/mL, the plates were visually checked for colony growth. Transformation of pYES2/CT-GFS yielded many colonies.

Colony PCR screening was employed on 8 colonies to identify bacterial colonies harboring the desired GFS construct. This involved amplifying by PCR the GFS gene from individual colonies using primers RO_193 and RO_194 with expected amplicon size of 982bp (**Table 1**) and visualizing the amplified products on an agarose gel. The presence of the vector was confirmed only for colony #1 (**Figure 7**), which was chosen for further validation.

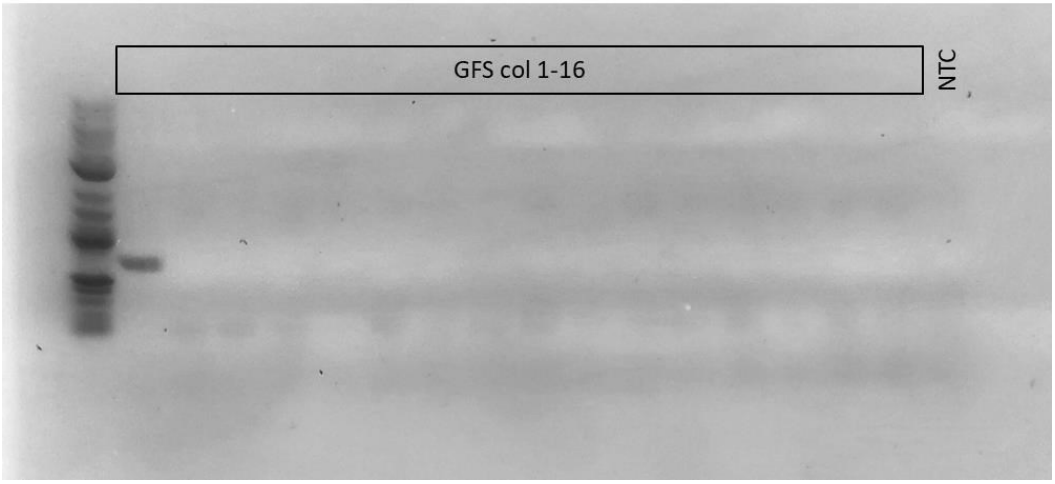

Figure 7. Colony PCR results for GFS. Figure 7 shows colony PCR results for GFS. Agarose gel electrophoresis image showing the PCR products from eight colonies. Colony #1 shows the expected band, confirming the presence of the GFS construct.

Colony #1, that tested positive for the GFS construct was inoculated into selective liquid LB culture media, allowing for growth and amplification of the bacterial cells containing the recombinant plasmid. After overnight growth in liquid culture, plasmid extraction was performed to isolate the recombinant plasmid pYES2/CT-GFS from the bacterial cells. The extracted plasmid was quantified at 80.1 ng/µL, and approximately 600 ng were used for restriction enzyme analysis to confirm the pYES2/CT-GFS plasmid structure. The restriction enzymes used, expected digestion pattern and location of restriction site are listed in **Table 2**.

Table 2. Restriction enzymes used to digest pYES2/CT-GFS & expected pattern.

Enzyme	Number of cuts	Fragments	Location
PvuI	2	4974 + 1901	Amp + backbone
ScaI	2	5982 + 893	Amp + Ura3
Hind III	2	6181 + 694	MCS + gene
XmnI	3	4353 + 1348 + 1174	backbone

As shown in **Figure 8**, the bands obtained partially match the expected pattern, with the low molecular weight band barely visible from the gel. Further attempts at plasmid extraction and digestion proved unsuccessful.

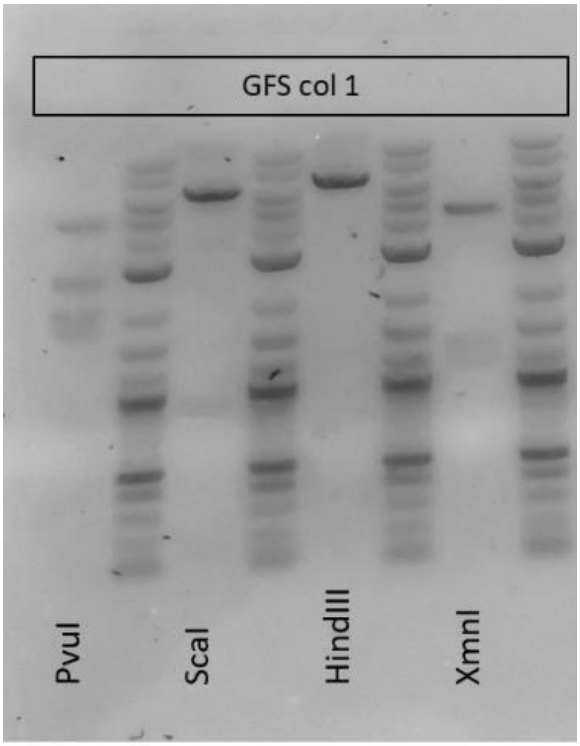

Figure 8. Gel image of pYES2/CT-GFS digestion. Figure 8 shows agarose gel electrophoresis image showing the digestion of the pYES2/CT-GFS plasmid with various restriction enzymes. The obtained bands partially match the expected pattern, with low molecular weight bands barely visible.

Cloning of Fucosyltransferase (FucT)

Fucosyltransferase was chosen for our studies because it is an enzyme involved in the biosynthesis of fucosylated glycoconjugates (**Figure 9**), which are important components of the fungal cell wall and play roles in pathogenesis and host-pathogen interactions. It catalyzes the transfer of fucose residues from an activated donor substrate, such as GDP-fucose, to specific acceptor molecules, which can be another sugar, lipid, protein, or existing glycan structure, through a glycosidic bond. This fucosylation modifies the structure and function of the acceptor molecule, contributing to the biosynthesis of complex fucose-containing glycans like those found in fungal cell walls.

The general reaction catalyzed by fucosyltransferase is: GDP-fucose + Acceptor molecule → Fucosylated product + GDP

Figure removed due to copyright restriction.

Figure 9. Reaction catalyzed by Fucosyltransferase (FucT) from https://pubs.rsc.org/en/content/articlelanding/2013/cs/c3cs60056d/unauth. Figure 9 shows a diagram of the reaction catalyzed by Fucosyltransferase (FucT), transferring fucose residues from GDP-fucose to acceptor molecules.

To clone FucT, the entire coding sequence was amplified from the cDNA of *R. arrhizus* using primers RO_199 and RO_200, as shown in **Table 1**, which contain restriction enzymes sites for subsequent cloning into the PYES/2CT vector. From the cDNA amplification, a band of 937 bp was expected, which was confirmed by gel electrophoresis (**Figure 10**).

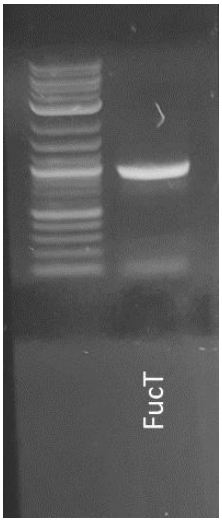

Figure 10. Gel image for PCR of FucT gene. Figure 10 shows agarose gel electrophoresis image showing the PCR amplification of the FucT gene. A single band of 937 bp confirms successful amplification.

To validate the amplicon, the FucT gene was purified from gel, quantified by Nanodrop and Sanger sequenced at AGRF to confirm sequence identity. Alignment of the sequencing results (**Figure 11**) with the expected coding sequence revealed a complete match between the amplified FucT gene and the expected sequence from the reference genome

.

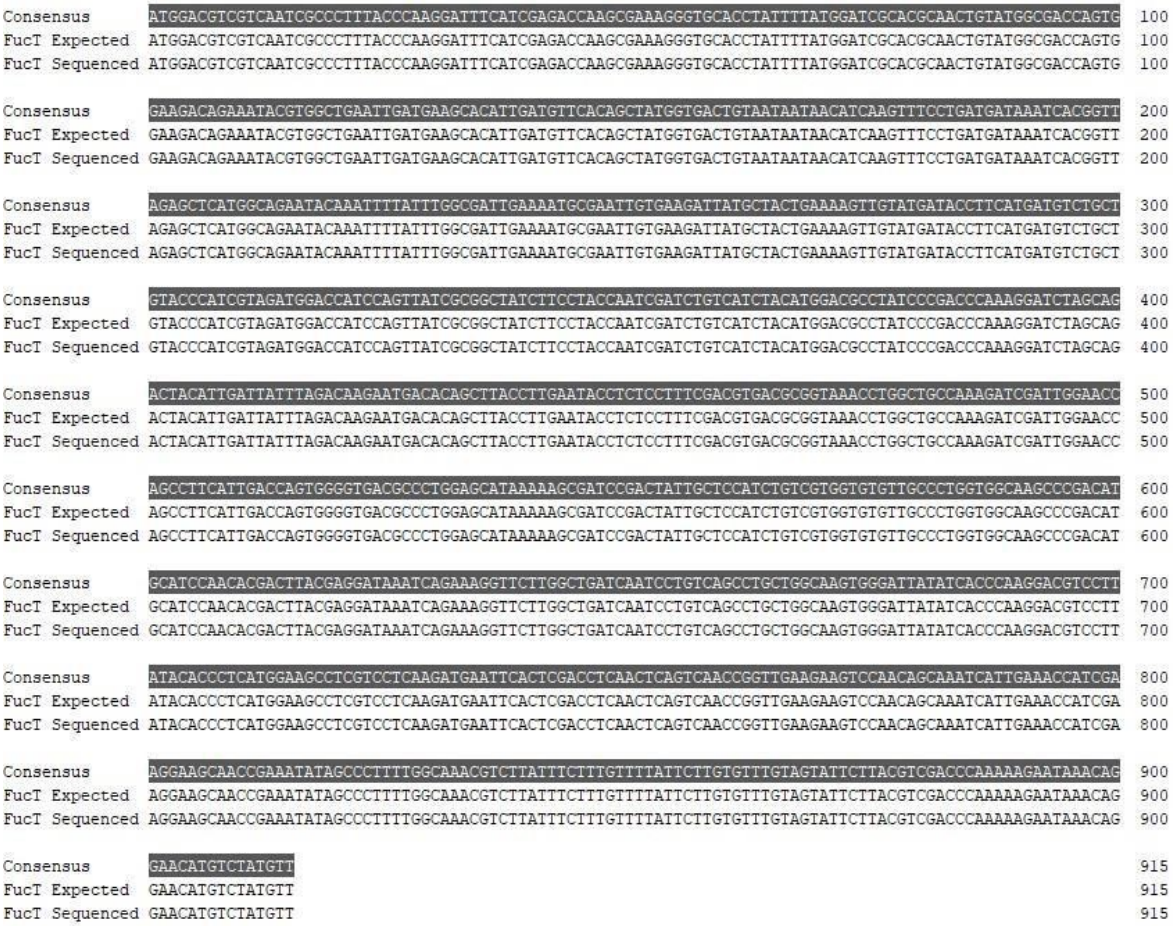

Figure 11. Alignment of FucT sequence. Figure 11 shows an alignment of the FucT sequence obtained from Sanger sequencing, showing a complete match with the reference genome.

After confirming the amplified coding sequence, 1 ug of material was used for restriction digestion with restriction enzymes BamHI and NotI to generate overhangs compatible with the expression vector pYES2/CT. Similarly to GFS, the digested FucT gene fragment was purified, quantified ligated with linearized vector backbone in a 3:1 insert:vector ratio. The ligation mixture containing the recombinant FucT vector, named pYES2/CT-FucT was transformed into DH5-Alpha cells chemically competent *E.coli* cells, resulting in many colonies which were then verified by colony PCR to identify positive colonies.

Eight colonies were screened and the presence of the vector could be confirmed only for colonies #5 and #13. Colony #5 was chosen for further investigation. Colony #5 was inoculated into selective liquid LB culture media and the recombinant plasmid pYES2/CT-FucT was extracted from the bacterial cells. The extracted plasmid was quantified at 43.9 ng/µL, and approximately 600 ng were used for restriction enzyme analysis to confirm the pYES2/CT-FucT plasmid structure. The restriction enzymes used, expected digestion pattern and location of restriction site are listed in **Table 3**.

Table 3. Restriction enzymes used to digest pYES2/CT-GFS.

Enzyme	Number of cuts	Fragments	Location
EcoRI	1	6830	Gene
PvuI	2	4929 + 1901	Amp + backbone
ScaI	2	5937 + 893	Amp + ura3
XmnI	3	4308 + 1348 + 1174	Backbone

As shown in **Figure 12**, no bands were obtained following digestion. Further attempts at plasmid extraction and digestion proved unsuccessful.

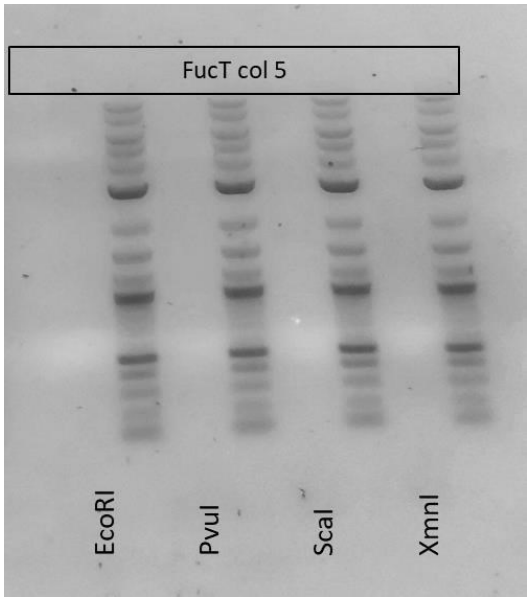

Figure 12. Gel image of pYES2/CT-FucT digestion. Figure 12 shows agarose gel electrophoresis image showing the digestion of the pYES2/CT-FucT plasmid with various restriction enzymes. No bands were visible.

Cloning of UDP-N-Acetylglucosamine pyrophosphorylase 1 (UAP1)

UDP-N-Acetylglucosamine pyrophosphorylase 1 (UAP1) was chosen for our studies because it is an enzyme involved in the biosynthesis of UDP-N-acetylglucosamine (UDP-GlcNAc), UAP1 generates the activated nucleotide sugar UDP-GlcNAc by transferring N-acetylglucosamine-1-phosphate onto UTP, releasing pyrophosphate (**Figure 13**). UDP-GlcNAc is then utilized by various glycosyltransferases as a donor substrate to incorporate N-acetylglucosamine into growing polysaccharide chains, including chitin, which is a major structural component of the fungal cell wall. By producing UDP-GlcNAc, UAP1 plays a crucial role in regulating the supply of this key precursor for cell wall biosynthesis in fungi.

It catalyzes the reversible reaction: UTP + N-Acetylglucosamine-1-phosphate ⇌ Pyrophosphate + UDP-N-Acetylglucosamine

Figure removed due to copyright restriction.

Figure 13. Reaction catalyzed by UDP-N-Acetylglucosamine pyrophosphorylase 1 (UAP1) from https://link.springer.com/referenceworkentry/10.1007/978-4-431-54240-7_153. Figure 13 shows as diagram of the reaction catalyzed by UDP-N-Acetylglucosamine pyrophosphorylase 1 (UAP1), converting UTP and N-Acetylglucosamine-1-phosphate to UDP-N-Acetylglucosamine and pyrophosphate.

To clone UAP1, the entire coding sequence was amplified from the cDNA of *R. arrhizus* using primers RO_195 and RO_196 (**Table 1**). As for the other genes, the primers contain BamHI and NotI restriction sites for subsequent cloning into the PYES/2CT vector. A band size of 1522 bp was expected, which was confirmed by gel electrophoresis (**Figure 14**).

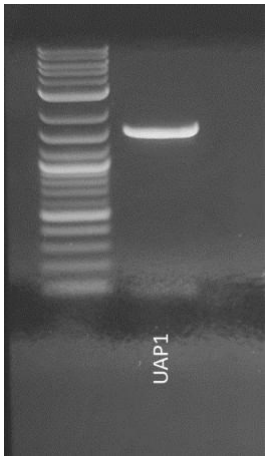

Figure 14. Gel image for PCR of UAP1 gene. Figure 14 shows agarose gel electrophoresis image showing the PCR amplification of the UAP1 gene. A single band of 1522 bp confirms successful amplification.

The amplified UAP1 gene was purified from gel, quantified, and sequenced. Alignment of the sequencing results with the expected coding sequence revealed a single SNP in the amplified UAP1 gene (**Figure 15**).

```
Consensus       ATGACTGTCTCCTCACTTCTTCCTATCAACGAAACTGAACTCCAAAGATTAAAAGAACTTTATGAAACAAACGGTCAAGGCCACGTATTCCGTTTCTTTG  100
UAP1 Expected   ATGACTGTCTCCTCACTTCTTCCTATCAACGAAACTGAACTCCAAAGATTAAAAGAACTTTATGAAACAAACGGTCAAGGCCACGTATTCCGTTTCTTTG  100
UAP1 Sequenced ATGACTGTCTCCTCACTTCTTCCTATCAACGAAACTGAACTCCAAAGATTAAAAGAACTTTATGAAACAAACGGTCAAGGCCACGTATTCCGTTTCTTTG  100

Consensus       AAACTCTGGAAGCAGAACAACAAGCTCAACTTGTGAAACAACTCCTTGAATTGGATGTTGAACGCCTGAATATTATCTATCGCAAGGCCATCGAAGGCGC  200
UAP1 Expected   AAACTCTGGAAGCAGAACAACAAGCTCAACTTGTGAAACAACTCCTTGAATTGGATGTTGAACGCCTGAATATTATCTATCGCAAGGCCATCGAAGGCGC  200
UAP1 Sequenced AAACTCTGGAAGCAGAACAACAAGCTCAACTTGTGAAACAACTCCTTGAATTGGATGTTGAACGCCTGAATATTATCTATCGCAAGGCCATCGAAGGCGC  200

Consensus       AGAGGCTGCCTCCTCCAGTCATCAGTTGGCACCTCTCCCCGAGACCGTGTTTGACTCTGTTCTGAAGGCTTCTGCTGAACAACTGCGTGAATGGGAGACG  300
UAP1 Expected   AGAGGCTGCCTCCTCCAGTCATCAGTTGGCACCTCTCCCCGAGACCGTGTTTGACTCTGTTCTGAAGGCTTCTGCTGAACAACTGCGTGAATGGGAGACG  300
UAP1 Sequenced AGAGGCTGCCTCCTCCAGTCATCAGTTGGCACCTCTCCCCGAGACCGTGTTTGACTCTGTTCTGAAGGCTTCTGCTGAACAACTGCGTGAATGGGAGACG  300

Consensus       ATCGGTTTGAGTCAAATTGCTCAAGGCAAGGTAGCTGTGATCTTGATGGCCGGTGGACAGGGCACTCGTCTGGGTTCCTCCGATCCCAAGGGCTGCTATA  400
UAP1 Expected   ATCGGTTTGAGTCAAATTGCTCAAGGCAAGGTAGCTGTGATCTTGATGGCCGGTGGACAGGGCACTCGTCTGGGTTCCTCCGATCCCAAGGGCTGCTATA  400
UAP1 Sequenced ATCGGTTTGAGTCAAATTGCTCAAGGCAAGGTAGCTGTGATCTTGATGGCCGGTGGACAGGGCACTCGTCTGGGTTCCTCCGATCCCAAGGGCTGCTATA  400

Consensus       ATATCAACTTACCTTCCAAAAAATCCCTTTTCCAATTACAAGCGGAACGTATCTTGCGCTTACAGGATATTGCCCGTCAATACAAGAAGCCTGGTAGCGG  500
UAP1 Expected   ATATCAACTTACCTTCCAAAAAATCCCTTTTCCAATTACAAGCGGAACGTATCTTGCGCTTACAGGATATTGCCCGTCAATACAAGAAGCCTGGTAGCGG  500
UAP1 Sequenced ATATCAACTTACCTTCCAAAAAATCCCTTTTCCAATTACAAGCGGAACGTATCTTGCGCTTACAGGATATTGCCCGTCAATACAAGAAGCCTGGTAGCGG  500

Consensus       TGACTGTATCATTCCTTGGTACATCATGACTTCCGGTCCCACTCATCGTCCTACATTTGAATTCTTTGAAAAAAATAACTTTTTCGGTCTTGAGAAGGAA  600
UAP1 Expected   TGACTGTATCATTCCTTGGTACATCATGACTTCCGGTCCCACTCATCGTCCTACATTTGAATTCTTTGAAAAAAATAACTTTTTCGGTCTTGAGAAGGAA  600
UAP1 Sequenced TGACTGTATCATTCCTTGGTACATCATGACTTCCGGTCCCACTCATCGTCCTACATTTGAATTCTTTGAAAAAAATAACTTTTTCGGTCTTGAGAAGGAA  600

Consensus       AATGTCATCTTTTTTGAGCAAGGTACTCTTCCTTGTTTAACTATGGATGGTAAGATTATTTTGGAAGCAAAGGATAAGGTGGCCATTGCTCCTGATGGTA  700
UAP1 Expected   AATGTCATCTTTTTTGAGCAAGGTACTCTTCCTTGTTTAACTATGGATGGTAAGATTATTTTGGAAGCAAAGGATAAGGTGGCCATTGCTCCTGATGGTA  700
UAP1 Sequenced AATGTCATCTTTTTTGAGCAAGGTACTCTTCCTTGTTTAACTATGGATGGTAAGATTATTTTGGAAGCAAAGGATAAGGTGGCCATTGCTCCTGATGGTA  700

Consensus       ATGGTGGTATTTACGCTGCAGTTTCTAACAAGGGCATCATCCGATCATTGAAAGAACGCGGTATTTTGTATTCACACTGTTACTGTGTCGACAACTGTCT  800
UAP1 Expected   ATGGTGGTATTTACGCTGCAGTTTCTAACAAGGGCATCATCCGATCATTGAAAGAACGCGGTATTTTGTATTCACACTGTTACTGTGTCGACAACTGTCT  800
UAP1 Sequenced ATGGTGGTATTTACGCTGCAGTTTCTAACAAGGGCATCATCCGATCATTGAAAGAACGCGGTATTTTGTATTCACACTGTTACTGTGTCGACAACTGTCT  800

Consensus       CGCTCGTGTAGCCGATCCGGTCTTTATCGGTTACTCTGTCTCCAAGGGAACCGACTGTGGTGTGAAGGTAGTGAGTAAGGCCTCTCCTGAAGAACCTGTA  900
UAP1 Expected   CGCTCGTGTAGCCGATCCGGTCTTTATCGGTTACTCTGTCTCCAAGGGAACCGACTGTGGTGTGAAGGTAGTGAGTAAGGCCTCTCCTGAAGAACCTGTA  900
UAP1 Sequenced CGCTCGTGTAGCCGATCCGGTCTTTATCGGTTACTCTGTCTCCAAGGGAACCGACTGTGGTGTGAAGGTAGTGAGTAAGGCCTCTCCTGAAGAACCTGTA  900

Consensus       GGTGTGGTCTGCGTTCGTGATGGTAAATACGGTGTGGTTGAATACTCTGAAATCTCTGAAGAAGTATCTCAAAAACGTAAAGAAGATGGCTCTCTTCAAT 1000
UAP1 Expected   GGTGTGGTCTGCGTTCGTGATGGTAAATACGGTGTGGTTGAATACTCTGAAATCTCTGAAGAAGTATCTCAAAAACGTAAAGAAGATGGCTCTCTTCAAT 1000
UAP1 Sequenced GGTGTGGTCTGCGTTCGTGATGGTAAATACGGTGTGGTTGAATACTYTGAAATCTCTGAAGAAGTATCTCAAAAACGTAAAGAAGATGGCTCTCTTCAAT 1000

Consensus       TTGGTGCTGCCAATATTGCCAATCATTTCTTTTCTACCGAATTCTTGGAACGTGTTCCTACTTTTGCTGATCAATTAGAATATCACATTGCTAAAAAGAA 1100
UAP1 Expected   TTGGTGCTGCCAATATTGCCAATCATTTCTTTTCTACCGAATTCTTGGAACGTGTTCCTACTTTTGCTGATCAATTAGAATATCACATTGCTAAAAAGAA 1100
UAP1 Sequenced TTGGTGCTGCCAATATTGCCAATCATTTCTTTTCTACCGAATTCTTGGAACGTGTTCCTACTTTTGCTGATCAATTAGAATATCACATTGCTAAAAAGAA 1100

Consensus       GATCAAGTACGTTGATCTTGAGACAGGAGAAGTGGTCGTACCCAAGTCTAACAGCGGCATGAAACTCGAATGCTTTGTGTTTGATGTCTTTCCTTATGCC 1200
UAP1 Expected   GATCAAGTACGTTGATCTTGAGACAGGAGAAGTGGTCGTACCCAAGTCTAACAGCGGCATGAAACTCGAATGCTTTGTGTTTGATGTCTTTCCTTATGCC 1200
UAP1 Sequenced GATCAAGTACGTTGATCTTGAGACAGGAGAAGTGGTCGTACCCAAGTCTAACAGCGGCATGAAACTCGAATGCTTTGTGTTTGATGTCTTTCCTTATGCC 1200

Consensus       CAACACTTTAGTGTACTCGAAGTGGATCGTAAAGAAGAGTTTTCTCCTCTCAAAAATGCCCCTGGATCAGGTGCTGATTGCCCAGAGACATCACGAAGAG 1300
UAP1 Expected   CAACACTTTAGTGTACTCGAAGTGGATCGTAAAGAAGAGTTTTCTCCTCTCAAAAATGCCCCTGGATCAGGTGCTGATTGCCCAGAGACATCACGAAGAG 1300
UAP1 Sequenced CAACACTTTAGTGTACTCGAAGTGGATCGTAAAGAAGAGTTTTCTCCTCTCAAAAATGCCCCTGGATCAGGTGCTGATTGCCCAGAGACATCACGAAGAG 1300

Consensus       ACATTGTGGCACAGCATGTTCGTTTTATTGAGGCAGCAGGTGGTAAGGTTTCGGGTGATGGTGACTTTGAAAAACTTCAGTTTGAAATCTCCCCTTGGGT 1400
UAP1 Expected   ACATTGTGGCACAGCATGTTCGTTTTATTGAGGCAGCAGGTGGTAAGGTTTCGGGTGATGGTGACTTTGAAAAACTTCAGTTTGAAATCTCCCCTTGGGT 1400
UAP1 Sequenced ACATTGTGGCACAGCATGTTCGTTTTATTGAGGCAGCAGGTGGTAAGGTTTCGGGTGATGGTGACTTTGAAAAACTTCAGTTTGAAATCTCCCCTTGGGT 1400

Consensus       CTCTTACTCTGGTGAAGGACTGAAGGAATATGTGGCTGGAAAGACGATTCGCATCCCTGCTATTATTGAAACAAAGGAAGACTTGATTCGTTTTGCTCAT 1500
UAP1 Expected   CTCTTACTCTGGTGAAGGACTGAAGGAATATGTGGCTGGAAAGACGATTCGCATCCCTGCTATTATTGAAACAAAGGAAGACTTGATTCGTTTTGCTCAT 1500
UAP1 Sequenced CTCTTACTCTGGTGAAGGACTGAAGGAATATGTGGCTGGAAAGACGATTCGCATCCCTGCTATTATTGAAACAAAGGAAGACTTGATTCGTTTTGCTCAT 1500
```

Figure 15. Alignment of UAP1 sequence. Figure 15 shows an alignment of the UAP1 sequence obtained from Sanger sequencing, showing a single SNP compared to the reference genome.

This result confirmed that the PCR amplification of the UAP1 gene was successful and accurate. The amplified UAP1 gene could therefore be confidently used for subsequent cloning. To do this, 1 ug of material was used for restriction digestion with BamHI and NotI restriction enzymes. The digested UAP1 gene fragment was purified, quantified and ligated into the linearized vpYES2/CT vector backbone, obtaining pYES2/CT-UAP1 which was transformed into DH5-Alpha cells chemically competent *E.coli* cells to yield few colonies. Colony PCR was used to screen 8 colonies, and was able to confirm the presence of the vector only in colonies #7 and #8 (**Figure 16**). Colony #7 was chosen for downstream reactions.

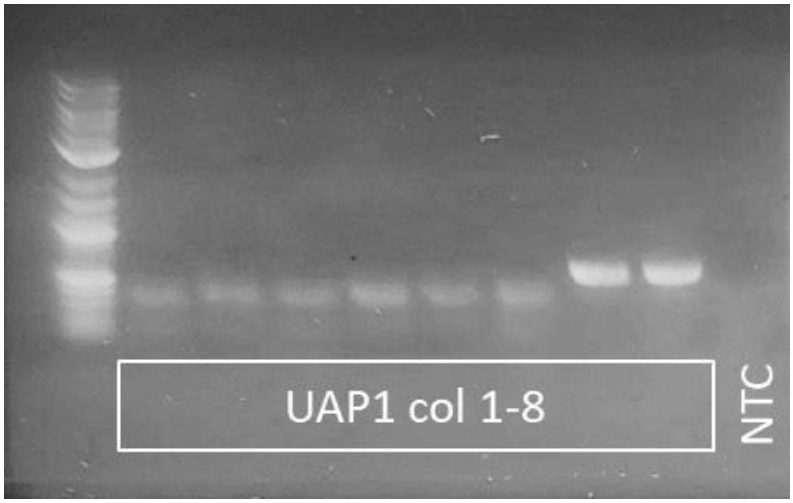

Figure 16. Colony PCR results for UAP1. Figure 16 shows a colony PCR results for UAP1. Agarose gel electrophoresis image showing the PCR products from eight colonies. Colonies #7 and #8 show the expected band, confirming the presence of the UAP1 construct.

The vector from colony # 7 was extracted from the bacterial cells and checked by restriction enzyme analysis to confirm the pYES2/CT-UAP1 plasmid structure. The restriction enzymes used, expected digestion pattern and location of restriction site are listed in **Table 4**.

Table 4. Restriction enzymes used to digest pYES2/CT-UAP1.

Enzyme	Number of cuts	Fragments	Location
Hind III	1	7415	MCS
EcoRI	2	6935 + 480	Gene
ScaI	2	6522 + 893	Amp + ura3
PvuI	3	3031 + 2483 + 1901	Gene + Amp + backbone

As shown in **Figure 17**, the bands obtained fully match the expected pattern, confirming the pYES2/CT-UAP1 vector.

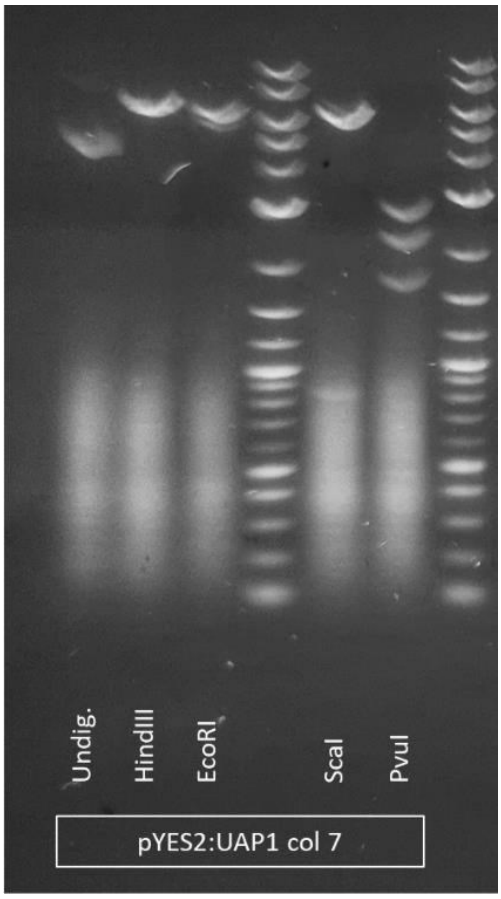

Figure 17. Gel image of pYES2/CT-UAP1 digestion. Figure 17 shows Agarose gel electrophoresis image showing the digestion of the pYES2/CT-UAP1 plasmid with various restriction enzymes. The obtained bands fully match the expected pattern.

As additional validation, the plasmid was also Sanger sequenced. Sequencing results showed that the insert had been successfully cloned in frame with the tags for purification with a 100% match to the expected sequence (**Figure 18**).

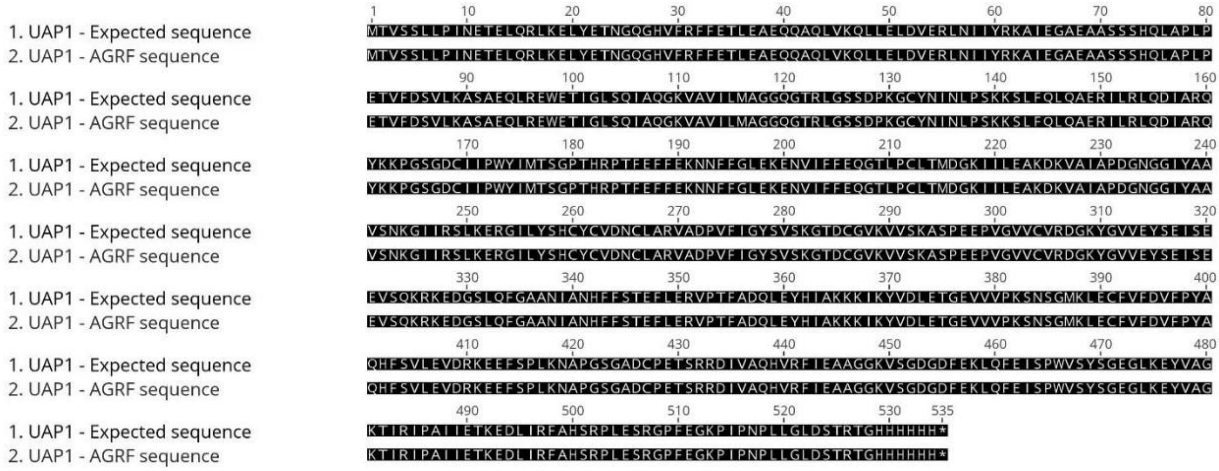

Figure 18. Sequence Result of UAP1 from Sanger Sequencing. Figure 18 shows an alignment of the UAP1 sequence obtained from Sanger sequencing, showing a 100% match with the expected sequence.

To ensure the long-term preservation and future use of the UAP1 clone, glycerol stocks were prepared, enabling the storage of the transformed bacterial cells at cryogenic temperatures.

Cloning of UDP-N-Acetylglucosamine pyrophosphorylase 2(UAP2)

Like UAP1, UDP-N-Acetylglucosamine pyrophosphorylase 2 (UAP2) was chosen for our studies because it is an enzyme involved in the biosynthesis of UDP-N-acetylglucosamine (UDP-GlcNAc), catalyzing the same reversible reaction (**Figure 13**).

To clone UAP2, the entire coding sequence was amplified from the cDNA of *R. arrhizus* using primers RO_197 and RO_198 which also primers contain BamHI and NotI restriction sites for subsequent cloning into the PYES/2CTvector. From the cDNA amplification, a band of 1528 bp was expected and successfully obtained (**Figure 19**).

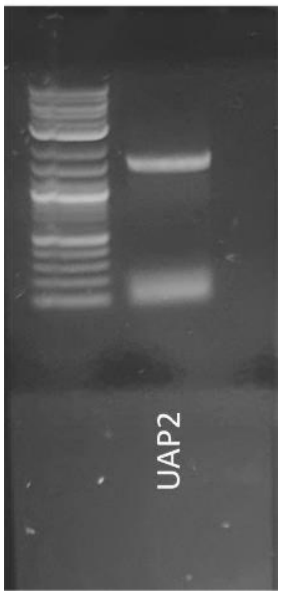

Figure 19. Gel image for PCR of UAP2 gene. Figure 19 shows agarose gel electrophoresis image showing the PCR amplification of the UAP2 gene. A single band of 1528 bp confirms successful amplification.To check amplicon sequence, the amplified UAP2 gene was purified from gel and Sanger sequenced, which confirmed that the correct gene had been amplified, with minimal discrepancies consisting of 4 SNPs compared to the reference genome (**Figure 20**).

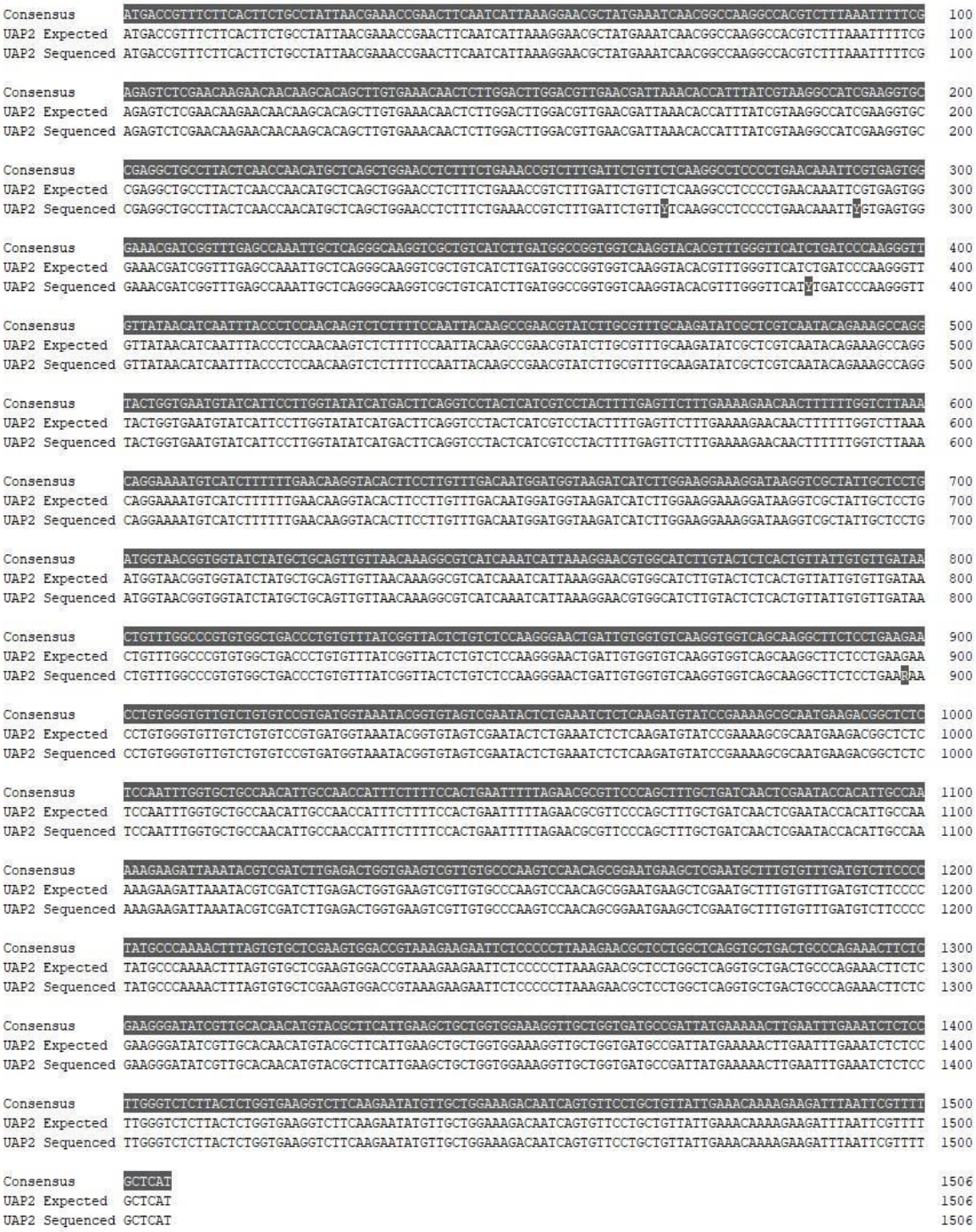

Figure 20. Alignment of UAP2 sequence. Figure 20 shows an alignment of the UAP2 sequence obtained from Sanger sequencing, showing four SNPs compared to the reference genome.

After confirming the amplified coding sequence, compatible overhangs for cloning were made by digestion of 1 ug of material with restriction enzymes BamHI and NotI. Digested material was purified, quantified and ligated into the linearized pYES2/CT backbone, obtaining the final recombinant pYES2/CT-UAP2 vector. The recombinant vector was transformed into DH5-Alpha cells chemically competent *E.coli* cells to ensure propagation. Following overnight growth at 37°C on selective media, the plates were visually checked for colony growth. Transformation of pYES2/CT-UAP2 yielded numerous colonies.

To identify bacterial colonies harboring the desired UAP2 construct, colony PCR screening was employed on 16 colonies. The amplified products were visualized on an agarose gel, confirming positive results for colonies #9 and #14 (**Figure 21**).

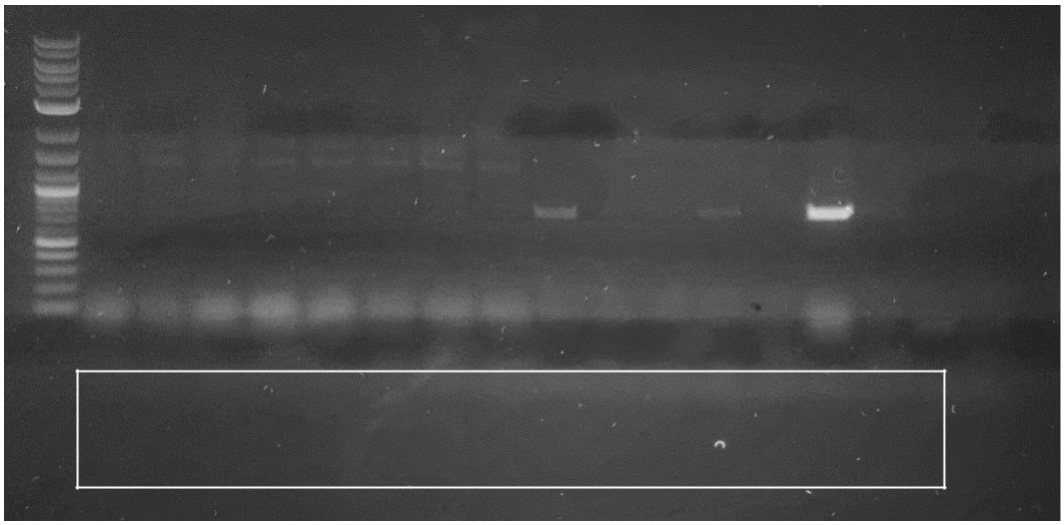

Figure 21. Colony PCR results for UAP2. Figure 21 shows a colony PCR results for UAP2. Agarose gel electrophoresis image showing the PCR products from 16 colonies. Colonies #9 and #14 show the expected band, confirming the presence of the UAP2 construct.

Both colonies #9 and #14 were chosen for further verification. To do this, the colonies were inoculated into selective liquid LB culture media for overnight growth and plasmid extraction.

Approximately 600 ng were used for restriction enzyme analysis. The restriction enzymes used, expected digestion pattern and location of restriction site are listed in **Table 5**.

Table 5. Restriction enzymes used to digest pYES2/CT-UAP2.

Enzyme	Number of cuts	Fragments	Location
EcoRI	1	7421	Gene
ScaI	2	6528 + 893	Amp + Ura3
PvuI	3	3031 + 2489 + 1901	Gene + amp + backbone

As shown in **Figure 22**, the bands obtained mostly matched the expected pattern for colony #9, however an additional band was identified in the digestion with ScaI. For colony #14, two additional bands are present following ScaI digestion. Patterns obtained with all other restriction enzymes matched expectations. Sanger sequencing attempts for further vector validation proved unsuccessful.

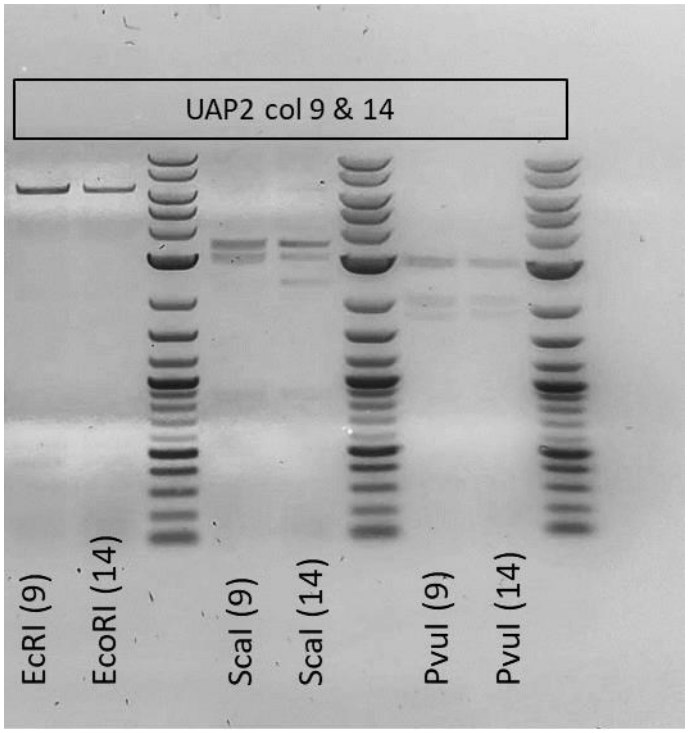

Figure 22. Gel image of pYES2/CT-UAP2 digestion. Figure 22 shows agarose gel electrophoresis image showing the digestion of the pYES2/CT-UAP2 plasmid with various restriction enzymes. The bands for colony #9 mostly match the expected pattern, while additional bands are seen for colony #14 following ScaI digestion.

DISCUSSION

Here we describe this approach, applied to the cloning of four essential enzymes in the biosynthesis of fungal cell wall components from pathogenic fungus R. arrhizus. The enzymes GDP-fucose synthase (GFS), fucosyltransferase FucT, UDP-N-acetylglucosamine pyrophosphorylase 1 (UAP1), and UDP-N-acetylglucosamine pyrophosphorylas2e (UAP2) were the focus of this study because they play unique roles in producing the fucose-containing polysaccharides and chitin that are critical components of the fungal cell wall. We chose the pYES2/CT expression vector, which is a versatile vector that may be used to express recombinant proteins in the yeast Saccharomyces cerevisiae. The plasmid vector contains a galactose-inducible GAL1 promoter for strict control of gene expression, while the C-terminal tags allow for visualization and isolation of the expressed proteins. Moreover, its auxotrophic markers and antibiotic resistance genes make it an easy-to-select and maintain transformant.

In the cloning procedure, the expression of the target genes was initiated from R. arrhizus cDNA by amplifying using specific primers with compatible restriction sites for further cloning into pYES2/CT vector. We confirmed the successful amplification of the corresponding gene fragments by agarose gel electrophoresis and purified and quantified the amplicons.

When we performed a Sanger sequencing of the amplified genes of GFS, FucT, and UAP2, we found out that that these genes were perfectly amplified, with reduced variation in comparison to the expected coding sequences. But there was a problem when the recombinant plasmids were extracted and verified. Even with several trials, it was not

possible to clone and transform the GFS, FucT, and UAP2 genes. There are a few reasons for this, which are highlighted below:

Inefficient ligation reactions: it is possible that the step of ligation that adds amplified gene segments into the plasmid vector isn't enough to initiate the process. There are simple processes that could have resulted in the production of low recombinant plasmid, including poor enzyme quality, low DNA end concentrations, and then suboptimal ligation conditions in most cases. But to enhance the efficiency of the ligation process, we need to either increase the ligation period, use more efficient ligases or oprimise the molar ratio of insert to vector.

Issues Transformation efficiency: When transformation efficiency is affected, it also has a negative impact on the introduction of recombinant plasmids into the host cells. Some things that could be causing this includes the competence of the host cells or the quality of the plasmid DNA. To increase the success rate of the transformation, we need to use highly competent cells with high DNA integrity.

Plasmid Stability and Maintenance: There are certain cases of instability and inability to maintain recombinant plasmids even after successful introduction into the host. Often, this is caused by high-copy plasmids adding metabolic load on the host, which causes it to loss plasmid or cause rearrangement. To increase plasmid stability, we can use low-copy plasmid vectors or stabilizing elements.

So, we had to stop the cloning of these genes, even when the cloning process was successful, characterization and expression it was important to get more understanding of fungal cell wall biosynthesis and potentially lead to the development of relevant antifungal

strategies that are focus on these vital pathways. To fix this issues would require systematic troubleshooting. However, when each step of the cloning process is optimized, it's possible to increase the chances of expressing these genes (GFS, FucT, and UAP2). Also, checking out alternative options like different expression systems, gene synthesis, and optimizing host conditions might give vital options on how to fix this problem.

For the amplified UAP1, it not only showed strong match with the reference sequence, but also confirmed the accuracy of the PCR amplification, but we also reached successful cloning and transformation as was shown in the plasmid digestion analysis and colony PCR screening. Also, we successfully isolated the recombinant pYES2/CT-UAP1 construct from bacterial transformants, which makes it easier to continue future studies on the characterization and expression of the UAP1 gene. However, the successful expression and purification of the enzyme (UAP1) helps in detailed study of biochemical and structural characterization, which could help understand the catalytic mechanism as well as the regulation. It will help strengthen the knowledge from previous research which have emphasized the importance of UAP1 in different biological processes. Research shows that UAP1 is important for glycosylation processes which is important for maintaining cell wall integrity and signaling in eukaryotic cells during nucleotide sugar metabolism pathway (Smith et al., 2015).

As confirmed by Johnson and colleagues (2018), we have it that changes in the activities of UAP1 can cause in changes in the cellular physiology, like changes in the structure of the glycan which generally affects the cell interaction and adhesion. Findings like this further emphasizes the potential value of UAP1 research in relation to the pathway of different disease, particularly those that include abnormalities in glycosylation.

There was a recent success in structural biology from Chen et al. (2020) where cryo-electron microscopy and Xray crystallography was used to reveal the detailed structure of glycosyltransferases. So, we have that the purification and production of UAP1 will give room for comparable structural analysis to clarify the active site dynamics of the enzyme and substrate selectivity. When we understand these features at the molecular level, it will help us build specific activators and inhibitors, which allows for therapeutic options during illnesses where the activity of UAP1 is not regulated.

CONCLUSION

Finally, we found that the UDP-N-acetylglucosamine pyrophosphorylase 1 (UAP1) gene was successfully cloned from Rhizopus arrhizus which is the pathogenic fungus in the pYES2/CT expression vector. But other attempts to express and clone other enzymes including fucosyltransferase (FucT), UDP-N-acetylglucosamine pyrophosphorylase 2 (UAP2) and GDP-fucose synthase (GFS) genes were unsuccessful because of some technical challenges during cloning. Since the UAP1 was successful, it gives room for future studies to characterize the recombinant enzyme and also understand what it does during the biosynthesis of an important precursor for the production of chitin in fungal cell walls. Proper structural and biochemical evaluation of UAP1 could give important details into the working process of the catalysts, regulation and the possibility as a target for producing antifungal drug s.

We would need to further troubleshoot and optimize the remaining genes of GFS, FucT, and UAP2, so that we can overcome the challenges that was encountered during cloning. Alternatively, we can use gene synthesis to analyze different hosts and expression systems, or we could optimize the cloning conditions so as to get functional recombinant constructs.

Given the central role of chitin and fucose-containing polysaccharides in the fungal cell wall, successful expression and characterization of these enzymes would provide significant insight into the biosynthesis of these important components. This work could eventfully open up the possibility to entirely new strategies in antifungal medicine that target these central pathways, thereby enabling us to treat and manage fungal infections better.

Just as one limitation, the present work was performed in S. cerevisiae and studies will now need to be carried out to confirm that ReBL simplifies labeling of glycoproteins in other fungi and at later stages in fungal cells. Because it is becoming increasingly difficult to detect effective anti-fungals, we must check how the process of fungal cell wall investment can identify novel therapeutic targets and address a world-wide pandemic associated with antifungal resistance.

REFERENCES

Adrio, J. L., & Demain, A. L. (2014). Microbial enzymes: tools for biotechnological processes. Biomolecules, 4(1), 117–139. https://doi.org/10.3390/biom4010117

Agarwal, P. K. (2018). A Biophysical Perspective on Enzyme Catalysis. Biochemistry, 58(6), 438–449. https://doi.org/10.1021/acs.biochem.8b01004

Bayer. (2022). Wheat Rust Diseases | Crop Science US. Bayer Crop Science Homepage |

Crop Science US. https://www.cropscience.bayer.us/articles/cp/wheat-rust-diseases#:~:text=According%20to%20the%20United%20Nations%20Food%20and%20Agriculture,70%20percent%20or%20more%20loss%20in%20wheat%20yield.

Benedict, K., & Park, B. J. (2014). Invasive fungal infections after natural disasters. Emerging infectious diseases, 20(3), 349–355. https://doi.org/10.3201/eid2003.131230

Brown, G. D., Denning, D. W., Gow, N. A., Levitz, S. M., Netea, M. G., & White, T. C. (2012).

Hidden killers:

Human fungal infections. Science Translational Medicine, 4(165), 165rv13.

CDC. (2023, July 31). Fungal Infections: Protect Your Health. Centers for Disease Control and Prevention. https://www.cdc.gov/

Chakrabarti, A., Das, A., Sharma, A., Panda, N., Das, S., Gupta, K. L., ... & Sakhuja, V. (2006). Ten years' experience in zygomycosis at a tertiary care centre in India. Journal of Infection, 52(5), 378-384.

Chen, Y., et al. (2020). "Structural insights into glycosyltransferases: Advances from X-ray crystallography and cryo-electron microscopy." Nature Structural & Molecular Biology, 27(7), 619-630.

Chen, X., & Chen, H. Y. H. (2021). Plant mixture balances terrestrial ecosystem C:N:P stoichiometry. Nature Communications, 12(1). https://doi.org/10.1038/s41467-021-24889-w

Cherney, D. Z. I., Zinman, B., Inzucchi, S. E., Koitka-Weber, A., Mattheus, M., von Eynatten, M., & Wanner, C. (2017). Effects of empagliflozin on the urinary albumin-to-creatinine ratio in patients with type 2 diabetes and established cardiovascular disease: an exploratory analysis from the EMPA-REG OUTCOME randomised, placebo-controlled trial. The lancet. Diabetes & endocrinology, 5(8), 610–621. https://doi.org/10.1016/S2213-8587(17)30182-1

Choi, J., Douglas, M., & Clark, M. (2018, March 18). Characteristics of Fungi. OpenStax. https://openstax.org/books/biology-2e/pages/24-1-characteristics-of-fungi

Deniaud-Bouët, E., Kervarec, N., Michel, G., Tonon, T., Kloareg, B., & Hervé, C. (2014). Chemical and enzymatic fractionation of cell walls from Fucales: insights into the structure of the extracellular matrix of brown algae. Annals of botany, 114(6), 1203–1216. https://doi.org/10.1093/aob/mcu096

Fang, F., Zhang, Y., Huang, X., Zhong, X., & Zhang, C. (2022). Secondary metabolites from fungus Rhizopus arrhizus: Structures and biological activities. Biomedicine & Pharmacotherapy, 146, 112407. https://doi.org/10.1016/j.biopha.2021.112407

Free, S. J. (2013). Fungal cell wall organization and biosynthesis. Advances in Genetics, 81, 33-82.

Fones, H. N., Bebber, D. P., Chaloner, T. M., Kay, W. T., Steinberg, G., & Gurr, S. J. (2020). Threats to global food security from emerging fungal and oomycete crop pathogens. Nature Food, 1(6), 332–342. https://doi.org/10.1038/s43016-020-0075-0

Gow, N. A. R., Latgé, J. P., & Munro, C. A. (2017). The fungal cell wall: Structure, biosynthesis, and function. Microbiology Spectrum, 5(3).

Grossart, H., Wyngaert, S., Kagami, M., Wurzbacher, C., Cunliffe, M., & Rojas-Jimenez, K. (2019). Fungi in aquatic ecosystems. Nature Reviews Microbiology, 17(6), 339-354. https://doi.org/10.1038/s41579-019-0175-8

Hesseltine, C. W. (1965). Tempeh—A Mold-Modified Indigenous Fermented Food Made from Soybeans and/or Cereals. Journal of Agricultural and Food Chemistry, 13(3), 279-283.

Hoermann, C., Benbow, M., Rottler-Hoermann, A., Lackner, T., Sommer, D., Receveur, J. & Müller, J. (2023). Factors influencing carrion communities are only partially consistent with

those of deadwood necromass. Oecologia, 201(2), 537-547. https://doi.org/10.1007/s00442-023-05327-8

Invitrogen (2009, November 30). pYES2/CT, pYES3/CT, and pYC2/CT: Yeast expression vectors with C-terminal tags and auxotrophic selection markers. CT No. V8251-20, Manual part No.: 25-0304.

Johnson, M., et al. (2018). "Impact of UAP1 activity on cellular physiology and glycan structures." Glycobiology, 28(5), 394-405.

Kashyap, D. R., Vohra, P. K., Chopra, S., & Tewari, R. (2001). Applications of pectinases in the commercial sector: a review. Bioresource technology, 77(3), 215-227. https://doi.org/10.1016/S0960-8524(00)00118-8

Kauffman, C. A. (2015). Zygomycosis: rethinking an opportunistic infection. Clinical Infectious Diseases, 41(2), 313-315.

Kumar, D., Kumar, L., Nagar, S., Mittal, A., Gupta, V. K., & Gupta, V. K. (2020). Microbial synthesis of biodiesel: a systematic investigation from strain selection to process optimization. Fuel, 276, 117806. https://doi.org/10.1016/j.fuel.2020.117806

Kwon-Chung, K. J., & Sugui, J. A. (2013). What do we know about the role of gliotoxin in the pathobiology of Aspergillus fumigatus? Medical Mycology, 51(6), 534-541.

Lairson, L. L., Henrissat, B., Davies, G. J., & Withers, S. G. (2008). Glycosyltransferases: structures, functions, and mechanisms. Annual Review of Biochemistry, 77, 521-555.

Latgé, J. P. (2007). The cell wall: A carbohydrate armour for the fungal cell. Molecular Microbiology, 66(2), 279-290.

Markets and Markets. (2021). Fumaric Acid Market by Type (Food Grade, Technical Grade), Application (Food & Beverages, Rosin Paper Sizes, UPS Resin, Alkyd Resins, Animal

Feed, Others), Form (Dry, Liquid), and Region - Global Forecast to 2027. https://www.marketsandmarkets.com/Market-Reports/fumaric-acid-market-95199594.html

Mélida, H., Sain, D., Stajich, J. E., & Bulone, V. (2015). Deciphering the uniqueness of Mucoromycotina cell walls by combining biochemical and phylogenomic approaches. Environmental microbiology, 17(5), 1649-1662.

Mendoza, L., Vitela, R., Voelz, K., Ibrahim, A.S., Voigt, K., Lee, S.C. (2015). Human Fungal Pathogens of Mucorales and Entomophthorales. Cold Spring Harbor Perspectives on Medicine, 5(4): a019562. https://perspectivesinmedicine.cshlp.org/content/5/4/a019562

Munro, C. A. (2013). Chitin and glucan, the yin and yang of the fungal cell wall, implications for antifungal drug discovery and therapy. Advances in Applied Microbiology, 83, 145-172.

Rauseo, A. M., Aljorayid, A., Olsen, M. A., Larson, L., Lipsey, K. L., Powderly, W. G., & Spec, A. (2021). Clinical predictive models of invasive Candida infection: A systematic literature review. Medical Mycology. https://doi.org/10.1093/mmy/myab043

Skiada, A., Pavleas, I., & Drogari-Apiranthitou, M. (2020). Epidemiology and Diagnosis of Mucormycosis: An Update. Journal of fungi (Basel, Switzerland), 6(4), 265. https://doi.org/10.3390/jof6040265

Varki, A., Cummings, R.D., Esko, J.D., et al., editors. Essentials of Glycobiology [Internet]. 4th edition. Cold Spring Harbor (NY): Cold Spring Harbor Laboratory Press; 2022. https://www.ncbi.nlm.nih.gov/books/NBK579918/

World Health Organization. (2022, October 25). WHO fungal priority pathogens list to guide research, development and public health action. World Health Organization (WHO). https://www.who.int/publications/i/item/9789240060241

World Health Organization. (2023, January 16). Neglected tropical diseases. World Health

Organization (WHO). https://www.who.int/news-room/questions-and-answers/item/neglected-tropical-diseases

Pandey, A., Soccol, C. R., Nigam, P., Brand, D., Mohan, R., & Roussos, S. (2000). Biotechnological potential of coffee pulp and coffee husk for bioprocesses. Biochemical Engineering Journal, 6(2), 153-162.

Precedence Research. (2023, February). Antifungal Drugs Market Size, Report By 2023 To 2032.

Precedence Research - Market Research Reports & Consulting Firm. https://www.precedenceresearch.com/antifungal-drugs-market

Ribes, J. A., Vanover-Sams, C. L., & Baker, D. J. (2000). Zygomycetes in human disease. Clinical Microbiology Reviews, 13(2), 236-301.

Singh, A. K., Singh, R., Joshi, S. R., Misra, A. (2021). Mucormycosis in COVID-19: A systematic review of cases reported worldwide and in India. Diabetes & Metabolic Syndrome: Clinical Research & Reviews, 15(4), 102146.

Spellberg, B., Edwards Jr, J., Ibrahim, A., & Filler, S. (2005). Mucormycosis: a turn of the century fungal infection. Clinical Microbiology Reviews, 18(3), 662-690.

Viana, C. (2021, September 10). Benefits of Fungi for the Environment and Humans. Chloride Free Foundation. https://chloridefree.org/en/benefits-of-fungi-for-the-environment-and-humans/

Vollmer, W., Blanot, D., & de Pedro, M. A. (2008). Peptidoglycan structure and architecture.

FEMS Microbiology Reviews, 32(2), 149-167.

Xu, X., Guo, L., Wang, Q., Li, F., & Zhou, L. (2019). Bioremediation of Heavy Metal Pollution Utilizing Rhizopus: Mechanisms and Application Prospects. Frontiers in Microbiology, 10, 2303. https://doi.org/10.3389/fmicb.2019.02303.

APPENDIX A

Glossary of cloning terms

TERM	DEFINITION
cDNA	It stands for complementary DNA, synthesised from a messenger RNA in a reaction called reverse transcription catalysed by the enzyme reverse transcriptase.
Cloning (biotechnology)	Refers to the process of making identical copies of DNA. It involves the following respectively amplification, digestion, ligation, transformation, plasmid extraction, glycerol stocks.
Competent cells	Are cells that have been treated to make them more permeable
Culture media	Are nutrient rich substances used to cultivate micro organisms such as bacteria etc.
Digestion	The process of cleaving DNA molecule using restriction enzymes
DNA ligase	This enzyme helps in DNA replication by joining fragments of DNA through phosphodiester bond. It is

	also used during cloning to add a DNA insert into a vector.

DNA polymerase	Is an enzyme involved in the synthesis of DNA molecule. It is used to amplify DNA fragments in large quantities.
***E. coli* (molecular biology)**	Is a species of bacteria used in laboratories for various experiments. I.e for transformation to act as host for foreign DNA for cloning.
Genomic DNA	Refers to the total DNA content present in the cell of an organism
Ligation	The process of joining two DNA fragments together using the enzyme DNA ligase.
Plasmid	Is a small, double stranded DNA molecule that is separate from the chromosomal DNA.
Quantification	Process of measuring the amount or concentration of DNA in a sample
Recombinant protein	Is a protein that had been produced through genetic manipulation
Restriction enzyme	Are enzymes that recognises specific DNA sequence and cleave them near recognition sites.

Resuspension	Refers to the process of bringing a dry or concentrated substance back into a solution

RNA	Is a molecule involved in various cellular processes e.g transcription
***S.cerevisiae* (molecular biology)**	Commonly known as baker's yeast, it plays a crucial role in cloning as host organism for heterologous protein expression due to its eukaryotic nature.
Transformation	Is a process by which foreign DNA is introduced into a host organism cell
Vector	Is a DNA molecule used as a vehicle to carry foreign genetic material into host organism cells
Vial	Is a small container used to store and transport liquids.